Fully discrete approximations to the time-dependent Navier-Stokes equations with a projection method in time and grad-div stabilization

Javier de Frutos* Bosco García-Archilla† Julia Novo‡

May 22, 2019

Abstract

This paper studies fully discrete approximations to the evolutionary Navier–Stokes equations by means of inf-sup stable H^1-conforming mixed finite elements with a grad-div type stabilization and the Euler incremental projection method in time. We get error bounds where the constants do not depend on negative powers of the viscosity. We get the optimal rate of convergence in time of the projection method. For the spatial error we get a bound $O(h^k)$ for the L^2 error of the velocity, k being the degree of the polynomials in the velocity approximation. We prove numerically that this bound is sharp for this method.

Keywords Incompressible Navier–Stokes equations; inf-sup stable finite element methods; grad-div stabilization; error constants independent of the viscosity; projection methods

1 Introduction

Let $\Omega \subset \mathbb{R}^d$, $d \in \{2,3\}$, be a bounded domain with polyhedral and Lipschitz boundary $\partial\Omega$. The incompressible Navier–Stokes equations model the conservation of linear momentum and the conservation of mass (continuity equation) by

$$\begin{aligned} \partial_t \boldsymbol{u} - \nu\Delta\boldsymbol{u} + (\boldsymbol{u}\cdot\nabla)\boldsymbol{u} + \nabla p &= \boldsymbol{f} && \text{in } (0,T)\times\Omega, \\ \nabla\cdot\boldsymbol{u} &= 0 && \text{in } (0,T)\times\Omega, \\ \boldsymbol{u}(0,\cdot) &= \boldsymbol{u}_0(\cdot) && \text{in } \Omega, \end{aligned} \tag{1}$$

*Instituto de Investigación en Matemáticas (IMUVA), Universidad de Valladolid, Spain. Research supported under grants MTM2016-78995-P (AEI/MINECO, ES) and VA024P17, VA105G18 (Junta de Castilla y León, ES) cofinanced by FEDER funds (frutos@mac.uva.es)

†Departamento de Matemática Aplicada II, Universidad de Sevilla, Sevilla, Spain. Research supported by Spanish MINECO under grant MTM2015-65608-P (bosco@esi.us.es)

‡Departamento de Matemáticas, Universidad Autónoma de Madrid. Spain Research supported under grants MTM2016-78995-P (AEI/MINECO, ES) and VA024P17 (Junta de Castilla y León, ES) cofinanced by FEDER funds (julia.novo@uam.es)

where $\boldsymbol{u}$ is the velocity field, p the kinematic pressure, $\nu > 0$ the kinematic viscosity coefficient, $\boldsymbol{u}_0$ a given initial velocity, and $\boldsymbol{f}$ represents the accelerations due to body forces acting on the fluid. The Navier–Stokes equations (1) are equipped with homogeneous Dirichlet boundary conditions $\boldsymbol{u} = \boldsymbol{0}$ on $\partial\Omega$.

We are interested in the case of small viscosity or, equivalently, high Reynolds number. For the spatial discretization a Galerkin finite element method with grad-div stabilization is considered for pairs of finite element spaces that satisfy a discrete inf-sup condition. Grad-div stabilization was originally proposed in [23] to improve the conservation of mass in finite element methods. It has been observed in the simulation of turbulent flows (see for example [36] and [45]) that using only grad-div stabilization led to reasonable results, in comparison with some other more complicated approaches, and produced stable (non-oscillating) simulations. The authors of [36] stated (see Summary Section) that the numerical studies showed that the grad-div term possesses a high importance. In the numerical experiments of [36] a constant stabilization parameter with value 1/2 was chosen for the grad-div term when using inf-sup stable elements. It must be noticed however that there is no clear-cut choice of the value of the grad-div stabilization parameter and the value depends on the physical units. Moreover, it is shown in [9], [39] that grad-div stabilization removes significant oscillations that appear in time dependent Navier-Stokes channel flow simulations over a step and in [20], [40] around a cylinder, although in [4] an example with a Taylor-Green vortex is presented where grad-div alone do not produce enough dissipation in the smallest scales. In [25] the authors proved error bounds for the evolutionary Oseen equations discretized with the Galerkin method and grad-div stabilization. An analysis of inf-sup stable elements with divergence-free approximations of the Navier–Stokes equations has been presented in [47]. There, error bounds independent of negative powers of ν were proved for the Galerkin method without any stabilization. Adding a grad-div stabilization term allows the use of more general, not necessarily divergence-free, finite elements. In [26], the analysis of [25] was extended to Navier-Stokes equations, obtaining again error bounds with constants that do not depend explicitly on inverse powers of the viscosity parameter. In [26] both the case in which the solution is assumed to be smooth enough and the case in which the solution is not assumed to satisfy nonlocal compatibility conditions are considered. The analysis covers the continuous in time case and the fully discrete case with the backward Euler method as time integrator.

We briefly comment on some other related works where stabilized finite element approximations to the Navier–Stokes equations are analyzed. The continuous interior penalty method was studied in [12], and local projection stabilization (LPS) method in [3, 21]. We want to remark that to our knowledge reference [12] is the first one where error bounds with constants independent on inverse powers of ν are obtained for the Navier-Stokes equations. In [10], error bounds for stabilized finite element approximations to the Navier–Stokes equations were obtained depending on exponentials of the $L^\infty(\Omega)$ norm of the gradient of the large eddies instead of the gradient of the full velocity $\boldsymbol{u}$, but limited to problems with periodic boundary conditions in rectangular domains. An analysis of a fully discrete method based on LPS in space and the Euler method in time was carried out in [2]. The error bounds in [2] are not independent of negative powers of ν. In [27] the method of [2] has been revisited and analyzed considering adding the fewest possible stabilization terms. Different schemes are obtained depending on which stabilization terms are added. For all of them, error bounds with constants independent on inverse powers of ν are obtained in the analysis in [27].

All error bounds in the above mentioned papers may depend implicitly on the viscosity through norms of the solution of the continuous problem on higher order Sobolev spaces. This will be also the case for the present paper and the rest of the related papers which we comment on further below.

In the present paper, we consider as time integrator the Euler incremental projection method. As stated in [38] "For high Reynolds number flows, splitting methods are more efficient computationally and competitive in accuracy compared to the mores expensive coupled methods". In [31] a subgrid stabilized projection method is applied for the simulation of 2D unsteady flows at high Reynolds numbers. In [8] a pressure-correction scheme for the incompressible Navier Stokes equations combining a discontinuous Galerkin approximation for the velocity and a standard continuous Galerkin approximation for the pressure is considered. The method is validated against a large set of classical two- and three-dimensional test cases covering a wide range of Reynolds numbers. In [22] the authors present numerical simulations for incompressible Navier-Stokes equations based on high-order discontinuous Galerkin discretizations and projection methods. The authors state that operator splitting techniques are well established solution approaches for incompressible Navier-Stokes equations that are particularly efficient for high Reynolds number flows. In [9] both sparse and standard grad-div stabilized projection methods are considered. It is shown that grad-div stabilization can increase the accuracy of projection methods for Navier-Stokes equations. As stated in [9] "An important future direction is to study grad-div stabilization, standard and sparse, for turbulent and higher Reynolds number flows, as there appears to be little in the literature on this topic both for projection and coupled time stepping schemes". Based on all these facts, we consider an interesting subject to get error bounds for projection methods applied to the Navier-Stokes equations with constants independent on inverse powers of the viscosity parameter.

An analysis of the semi-discretization in time with the Euler incremental scheme can be found in [42]. On the other hand, the Euler incremental scheme with a spatial discretization based on inf-sup stable mixed finite elements and a semi-implicit treatment of the nonlinear term has been analyzed in [33], where the authors get optimal error bounds. In the present paper, we follow the ideas in [33] with the main difference that our aim is to get bounds with constants independent on inverse powers of the viscosity, which was not intended in [33]. For this purpose, as mentioned above, we add a grad-div stabilization term to the spatial Galerkin discretization. We notice that error constants independent of the viscosity may also imply other practical consequences (besides the obvious one of smaller errors) as the following words from [11] aptly point out: "The importance of stabilization in the high Reynolds number regime from fractional-step methods was illustrated numerically in [31] for Navier-Stokes flows, showing that pressure-projection methods can fail to converge in the high Reynolds number regime unless some stabilization is applied".

In the present paper, for the Navier-Stokes equations, we get the optimal rate of convergence in time of order Δt, Δt being the size of the time step, for the errors in the L^2 norm of the velocity, the L^2 norm of the divergence of the velocity and a discrete in time L^2 norm of the pressure. Due to the requirement of error constants independent on the Reynolds number, the error in the pressure is obtained under the assumption $\Delta t \leq Ch^{d/2+1}$, $k \geq d/2+1$, d being the spatial dimension, and k being the degree of the polynomials in the velocity space, as opposed to [33], where the dependence of error constants on the Reynolds number allow for the weaker assumption $\Delta t \leq Ch^{1/2}$. Numerical experiments in Section 4 suggest that the restriction $\Delta t \leq Ch^{d/2+1}$ is not sharp in practice and that it is only needed in the proofs due to the technicalities of the analysis. For the spatial error we get a bound $O(h^k)$ for the L^2 error of the velocity, k being the degree of the polynomials in the velocity approximation. This error bound is suboptimal in space compared to other methods in the literature although we prove numerically that the bound is sharp for this method. Assuming enough regularity for the solution, error bounds of size $O(h^{k+1/2})$ have been proved in [12], [27] using continuous interior penalty stabilization and local projection stabilization, respectively. Although one might expect order $k+1$ for the L^2 error of the velocity this is one of the open problems that can be found in reference [37].

Error bounds for projection methods with constants independent of the Reynolds number were also obtained in [11] (which, to our knowledge, it is the first paper analyzing projection methods obtaining such bounds). In [11] the authors proved error bounds for the Euler incremental projection method and the continuous interior penalty finite element method in space with equal order elements for velocity and pressure (analyzed in [13] for stationary Oseen equations). However as opposed to the present paper, error bounds in [11] are obtained for the transient Oseen equations. Also, following [14], in [11] the authors proved a bound for a discrete in time primitive of the pressure instead of the stronger discrete in time L^2 norm of the pressure as in the present paper. The idea of getting a bound for the time-average of the pressure error considerably simplifies the pressure error analysis with respect to the standard $L^2(0,T;L^2(\Omega))$ norm (or its discrete counterpart) in which the pressure is usually bounded. Let us observe that in [11], for methods where the pressure is treated explicitly, a condition of type $Ch \leq \Delta t$ is required in the error analysis.

Related to the present paper also is [4], where a method with LPS streamline-upwind stabilization plus grad-div stabilization in space and a BDF2 projection method in time was analyzed. In the first part of [4] error bounds with constants independent on inverse powers of ν are obtained. However, the bounds depend on $\|\boldsymbol{u}_h\|_{L^\infty(L^\infty)}$, $\boldsymbol{u}_h$ being the approximation to the velocity, and no a priori bounds for this norm are proved. Moreover, the error bounds for the velocity are only $O(\Delta t)$ instead of $O((\Delta t)^2)$ and no error bounds for the pressure are proved. In the second part of [4] the authors get optimal bounds of order $O((\Delta t)^2)$ for the velocity (although only $O(\Delta t)$ for the pressure) although this is done at the price of error constants depending on ν^{-1}.

We now comment on other related works dealing with projection methods. In [43], [44], [48], [49] the analysis of the semidiscretization in time by Euler non incremental method is carried out. In [18] the stability of the Euler non incremental method with non inf-sup stable mixed finite elements was considered. Some a priori bounds for the velocity and pressure approximations are obtained but no error bounds were proved. In [6] the Euler non incremental scheme together with both non inf-sup stable and inf-sup stable elements was analyzed and in the non inf-sup stable case a local projection type stabilization is required. As opposed to this, no stabilization is added in [28], [29], where we obtained error bounds for a modified Euler non-incremental method for non inf-sup stable elements for evolutionary Stokes and Navier-Stokes equations. In [41] a stabilized version of the Euler incremental method for non inf-sup stable elements is proposed although no bounds are proved. In [24] the applicability of weighted essentially non-oscillatory (WENO) finite difference schemes for the simulation of incompressible flows is explored in conjunction with several non-incremental and incremental projection methods. A pressure stabilization PetrovGalerkin (PSPG) type of stabilization is introduced in [24] for the incremental schemes to account for the violation of the discrete inf-sup condition. We also want to refer to [32] for an overview on projection methods.

Altogether, in all the mentioned works, apart from [11] and [4], only stability aspects of the methods are studied or error bounds are proved but with constants in the error bounds depending on inverse powers of the viscosity parameter. Then, our aim in this paper is, as in [4], to fill in some sense the existing gap in the numerical analysis of getting bounds for the time-dependent incompressible Navier-Stokes equations with projection methods in time for high Reynolds numbers.

The outline of the paper is as follows. In Section 2 we introduce some notation. In Section 3 we prove the error bounds of the method. The main results are Theorem 1 that gathers the velocity bounds and which statement can be found at the end of Subsection 3.1, and Theorem 2, with the error bound for the pressure, which is located at the end of subsection 3.2. Some numerical results are presented in Section 4.

2 Preliminaries and notation

Throughout the paper, $W^{s,p}(D)$ will denote the Sobolev space of real-valued functions defined on a domain $D \subset \mathbb{R}^d$, $d = 2, 3$ with distributional derivatives of order up to s in $L^p(D)$. These spaces are endowed with the usual norm denoted by $\|\cdot\|_{W^{s,p}(D)}$. If s is not a positive integer, $W^{s,p}(D)$ is defined by interpolation [1]. In the case $s = 0$, it is $W^{0,p}(D) = L^p(D)$. As it is standard, $W^{s,p}(D)^d$ will be endowed with the product norm and, since no confusion can arise, it will be denoted again by $\|\cdot\|_{W^{s,p}(D)}$. The case $p = 2$ will be distinguished by using $H^s(D)$ to denote the space $W^{s,2}(D)$. The space $H_0^1(D)$ is the closure in $H^1(D)$ of the set of infinitely differentiable functions with compact support in D. For simplicity, $\|\cdot\|_s$ (resp. $|\cdot|_s$) is used to denote the norm (resp. seminorm) both in $H^s(\Omega)$ or $H^s(\Omega)^d$. The exact meaning will be clear by the context. The inner product of $L^2(\Omega)$ or $L^2(\Omega)^d$ will be denoted by $(\cdot,\cdot)$ and the corresponding norm by $\|\cdot\|_0$. The norm of the space of essentially bounded functions $L^\infty(\Omega)$ will be denoted by $\|\cdot\|_\infty$. For vector-valued functions, the same conventions will be used as before. The norm of the dual space $H^{-1}(\Omega)$ of $H_0^1(\Omega)$ is denoted by $\|\cdot\|_{-1}$. As usual, $L^2(\Omega)$ is always identified with its dual, so one has $H_0^1(\Omega) \subset L^2(\Omega) \subset H^{-1}(\Omega)$ with compact injection. For a given Banach space W, $L^p(0,T,W)$ denotes the corresponding Bochner space of functions defined on the time interval (0,T) with values in W. The norm in $L^p(0,T,W)$ will be denoted by $\|\cdot\|_{L^p(W)}$. When no confusion can arise we will frequently drop the dependence of the norms of the domain Ω.

Using the function spaces $V = H_0^1(\Omega)^d$ and

$$Q = L_0^2(\Omega) = \left\{q \in L^2(\Omega) : (q, 1) = 0\right\},$$

and assuming that $\boldsymbol{f} \in L^2(0, T, H^{-1}(\Omega)^d)$, the weak formulation of problem (1) is as follows: Find $(\boldsymbol{u}, p) \in \left[L^2(0, T, V) \cap L^\infty(0, T, L^2(\Omega)^d)\right] \times L^2(0, T, Q)$ such that for all $(\boldsymbol{v}, q) \in V \times Q$,

$$\langle \partial_t \boldsymbol{u}, \boldsymbol{v} \rangle + \nu(\nabla \boldsymbol{u}, \nabla \boldsymbol{v}) + ((\boldsymbol{u} \cdot \nabla)\boldsymbol{u}, \boldsymbol{v}) - (\nabla \cdot \boldsymbol{v}, p) + (\nabla \cdot \boldsymbol{u}, q) = < \boldsymbol{f}, \boldsymbol{v} >,$$

with $\boldsymbol{u}(0, \cdot) = \boldsymbol{u}_0(\cdot)$ in Ω. Here, $\langle \cdot, \cdot \rangle$ stands for the duality paring between H_0^1 and H^{-1}. Notice that the above relation has sense with $\partial_t \boldsymbol{u} \in L^1(0, T, H^{-1}(\Omega)^d)$ (see e.g.,[19, § 8]). Later, however, $(\boldsymbol{u}, p)$ will be required to be more regular, so that $\boldsymbol{f}$ will also be more regular. Consequently, $\langle \cdot, \cdot \rangle$ will be replaced by $(\cdot, \cdot)$.

The Hilbert space

$$H^{\text{div}} = \{\boldsymbol{u} \in L^2(\Omega)^d \ \mid \ \nabla \cdot \boldsymbol{u} = 0, \, \boldsymbol{u} \cdot \mathbf{n}|_{\partial\Omega} = 0\}$$

will be endowed with the inner product of $L^2(\Omega)^d$ and the space

$$V^{\text{div}} = \{\boldsymbol{u} \in V \ \mid \ \nabla \cdot \boldsymbol{u} = 0\}$$

with the inner product of V.

Let $\Pi \ : \ L^2(\Omega)^d \to H^{\text{div}}$ be the Leray projector that maps each function in $L^2(\Omega)^d$ onto its divergence-free part (see e.g. [19, Chapter IV]. The Stokes operator in Ω is given by

$$A \ : \ \mathcal{D}(A) \subset H^{\text{div}} \to H^{\text{div}}, \quad A = -\Pi\Delta, \quad \mathcal{D}(A) = H^2(\Omega)^d \cap V^{\text{div}}.$$

The following Sobolev's embedding [1] will be used in the analysis: For $1 \le p < d/s$ let q be such that $\frac{1}{q} = \frac{1}{p} - \frac{s}{d}$. There exists a positive constant C such that

$$\|v\|_{L^{q'}(\Omega)} \le C\|v\|_{W^{s,p}(\Omega)}, \quad \frac{1}{q'} \ge \frac{1}{q}, \quad v \in W^{s,p}(\Omega). \tag{2}$$

If $p > d/s$ the above relation is valid for $q' = \infty$. A similar embedding inequality holds for vector-valued functions.

Let $V_h \subset V$ and $Q_h \subset Q$ be two families of finite element spaces composed of piecewise polynomials of degrees at most k and l, respectively, that correspond to a family of partitions $\mathcal{T}_h$ of Ω into mesh cells with maximal diameter h. For simplicity, we restrict ourselves to meshes consisting of triangles/tetrahedra although the bounds of the paper equally hold for quadrilaterals/hexahedra. In this paper, we will only consider pairs of finite element spaces satisfying a discrete inf-sup condition,

$$\inf_{q_h \in Q_h} \sup_{\boldsymbol{v}_h \in V_h} \frac{(\nabla \cdot \boldsymbol{v}_h, q_h)}{\|\nabla \boldsymbol{v}_h\|_0 \|q_h\|_0} \ge \beta_0, \tag{3}$$

with $\beta_0 > 0$, a constant independent of the mesh size h. Since the error bounds for the pressure depend both on the mixed finite element used and on the regularity of the solution, and in general it will be assumed that $p \in Q \cap H^k(\Omega)$ with $l \ge k-1$, in the sequel the error bounds will be written depending only on k. For example, for the MINI element it is $k = l = 1$ and for the Hood–Taylor element one has $l = k - 1$.

It will be assumed that the family of meshes is quasi-uniform and that the following inverse inequality holds for each $\boldsymbol{v}_h \in V_h$, see e.g., [17, Theorem 3.2.6],

$$\|\boldsymbol{v}_h\|_{W^{m,p}(K)} \leq C_{\text{inv}} h_K^{n-m-d\left(\frac{1}{q}-\frac{1}{p}\right)} \|\boldsymbol{v}_h\|_{W^{n,q}(K)}, \tag{4}$$

where $0 \leq n \leq m \leq 1$, $1 \leq q \leq p \leq \infty$, and h_K is the size (diameter) of the mesh cell $K \in \mathcal{T}_h$.

The space of discrete divergence-free functions is denoted by

$$V_h^{\text{div}} = \{\boldsymbol{v}_h \in V_h \mid (\nabla \cdot \boldsymbol{v}_h, q_h) = 0 \quad \forall q_h \in Q_h\},$$

and by $A_h^{\text{div}} : V_h^{\text{div}} \to V_h^{\text{div}}$ we denote the following linear operator

$$(A_h^{\text{div}} \boldsymbol{v}_h, \boldsymbol{w}_h) = (\nabla \boldsymbol{v}_h, \nabla \boldsymbol{w}_h) \quad \forall \boldsymbol{v}_h, \boldsymbol{w}_h \in V_h^{\text{div}}.$$

Note that from this definition, it follows that for $\boldsymbol{v}_h \in V_h^{\text{div}}$,

$$\|(A_h^{\text{div}})^{1/2} \boldsymbol{v}_h\|_0 = \|\nabla \boldsymbol{v}_h\|_0, \quad \|\nabla (A_h^{\text{div}})^{-1/2} \boldsymbol{v}_h\|_0 = \|\boldsymbol{v}_h\|_0.$$

We also denote by $A_h : V_h \to V_h^{\text{div}}$ the linear operator

$$(A_h \boldsymbol{v}_h, \boldsymbol{w}_h) = (\nabla \boldsymbol{v}_h, \nabla \boldsymbol{w}_h) \quad \forall \boldsymbol{v}_h \in V_h, \boldsymbol{w}_h \in V_h^{\text{div}}.$$

Additionally, two linear operators $C_h : V_h \to V_h^{\text{div}}$ and $D_h : L^2(\Omega) \to V_h^{\text{div}}$ are defined by

$$\begin{aligned}(C_h \boldsymbol{v}_h, \boldsymbol{w}_h) &= (\nabla \cdot \boldsymbol{v}_h, \nabla \cdot \boldsymbol{w}_h) \quad \forall \boldsymbol{v}_h \in V_h, \boldsymbol{w}_h \in V_h^{\text{div}}, \\ (D_h p, \boldsymbol{v}_h) &= -(p, \nabla \cdot \boldsymbol{v}_h) \qquad \forall \boldsymbol{v}_h \in V_h^{\text{div}}.\end{aligned}$$

Denoting by π_h the $H^1(\Omega)$ projection onto Q_h, one has that for $m = 0, 1$:

$$\|q - \pi_h q\|_m \leq C h^{j+1-m} \|q\|_{j+1} \quad \forall q \in H^{j+1}(\Omega), \quad j = 0, \ldots, l. \tag{5}$$

In the error analysis, the Poincaré–Friedrichs inequality

$$\|\boldsymbol{v}\|_0 \leq C \|\nabla \boldsymbol{v}\|_0 \quad \forall \boldsymbol{v} \in H_0^1(\Omega)^d,$$

will be used.

In the sequel, $I_h \boldsymbol{u} \in V_h$ will denote the Lagrange interpolant of a continuous function $\boldsymbol{u}$. The following bound can be found in [7, Theorem 4.4.4]

$$|\boldsymbol{u} - I_h \boldsymbol{u}|_{W^{m,p}(K)} \leq c_{\text{int}} h^{n-m} |\boldsymbol{u}|_{W^{n,p}(K)}, \quad 0 \leq m \leq n \leq k+1, \tag{6}$$

where $n > d/p$ when $1 < p \leq \infty$ and $n \geq d$ when $p = 1$.

In the analysis, the Stokes problem

$$\begin{aligned}-\nu \Delta \boldsymbol{u} + \nabla p &= \boldsymbol{g} \quad \text{in } \Omega, \\ \boldsymbol{u} &= \boldsymbol{0} \quad \text{on } \partial\Omega, \\ \nabla \cdot \boldsymbol{u} &= 0 \quad \text{in } \Omega,\end{aligned} \tag{7}$$

will be considered. If we denote by $(\boldsymbol{u}_h, p_h) \in V_h \times Q_h$ the mixed finite element approximation to (7) following [30], one has the estimates

$$\|\boldsymbol{u}-\boldsymbol{u}_h\|_1 \le C\left(\inf_{\boldsymbol{v}_h\in V_h}\|\boldsymbol{u}-\boldsymbol{v}_h\|_1+\nu^{-1}\inf_{q_h\in Q_h}\|p-q_h\|_0\right), \tag{8}$$

$$\|p-p_h\|_0 \le C\left(\nu\inf_{\boldsymbol{v}_h\in V_h}\|\boldsymbol{u}-\boldsymbol{v}_h\|_1+\inf_{q_h\in Q_h}\|p-q_h\|_0\right), \tag{9}$$

$$\|\boldsymbol{u}-\boldsymbol{u}_h\|_0 \le Ch\left(\inf_{\boldsymbol{v}_h\in V_h}\|\boldsymbol{u}-\boldsymbol{v}_h\|_1+\nu^{-1}\inf_{q_h\in Q_h}\|p-q_h\|_0\right). \tag{10}$$

It can be observed that the error bounds for the velocity depend on negative powers of ν.

For the analysis, we will use a projection of $(\boldsymbol{u}, p)$ into $V_h \times Q_h$ with optimal bounds which do not depend on ν. In [25], [26] a projection with this property was introduced. Let $(\boldsymbol{u}, p)$ be the solution of the Navier–Stokes equations (1) with $\boldsymbol{u} \in V \cap H^{k+1}(\Omega)^d$, $p \in Q \cap H^k(\Omega)$, $k \ge 1$, for $t \ge 0$ the pair $(\boldsymbol{u}, 0)$ is the solution of the Stokes problem (7) with right-hand side

$$\boldsymbol{g} = \boldsymbol{f} - \partial_t\boldsymbol{u} - (\boldsymbol{u}\cdot\nabla)\boldsymbol{u} - \nabla p.$$

Denoting the corresponding Galerkin approximation in $V_h \times Q_h$ by $(\boldsymbol{s}_h, l_h)$, that is

$$\nu(\nabla\boldsymbol{s}_h, \nabla\boldsymbol{v}_h) - (l_h, \nabla\cdot\boldsymbol{v}_h,) + (\nabla\cdot\boldsymbol{s}_h, q_h) = (\boldsymbol{g}, \boldsymbol{v}_h),$$

for all $(\boldsymbol{v}_h, q_h) \in V_h \times Q_h$, one obtains from (8)–(10)

$$\|\boldsymbol{u}-\boldsymbol{s}_h\|_0 + h\|\boldsymbol{u}-\boldsymbol{s}_h\|_1 \le Ch^{j+1}\|\boldsymbol{u}\|_{j+1}, \quad 0\le j\le k, \tag{11}$$

$$\|l_h\|_0 \le C\nu h^j\|\boldsymbol{u}\|_{j+1}, \quad 0\le j\le k, \tag{12}$$

where the constant C does not depend on ν.
Remark 1 Assuming that $\partial_t\boldsymbol{u} \in H^k(\Omega)^d \cap V$ and considering (7) with

$$\boldsymbol{g} = \partial_t\left(\boldsymbol{f} - \partial_t\boldsymbol{u} - (\boldsymbol{u}\cdot\nabla)\boldsymbol{u} - \nabla p\right) = -\nu\nabla\boldsymbol{u}_t,$$

one can derive an error bound of the form (11) also for $\partial_t(\boldsymbol{u}-\boldsymbol{s}_h)$.

Following [16], one can also obtain the following bound for $\boldsymbol{s}_h$

$$\|\nabla(\boldsymbol{u}-\boldsymbol{s}_h)\|_\infty \le C\|\nabla\boldsymbol{u}\|_\infty, \tag{13}$$

where C does not depend on ν. Let us observe that the assumption

$$\boldsymbol{u} \in L^\infty(0,T;W^{1,\infty}(\Omega)^d)$$

is also required in other related references as [12], [3], [26] and [4].

Since $\|I_h(\boldsymbol{u})\|_\infty \le C\|\boldsymbol{u}\|_\infty$ for some $C>0$, one can write

$$\|\boldsymbol{s}_h\|_\infty \le \|\boldsymbol{s}_h - I_h(\boldsymbol{u})\|_\infty + \|I_h(\boldsymbol{u})\|_\infty \le C_{\rm inv}h^{-d/2}\|\boldsymbol{s}_h - I_h(\boldsymbol{u})\|_0 + C\|\boldsymbol{u}\|_\infty,$$

where in the last inequality inverse inequality (4) has been applied. Applying (6), (11), (2) and (13) one gets

$$\|\boldsymbol{s}_h\|_\infty \le C_\infty\|\boldsymbol{u}\|_2, \quad \|\nabla\boldsymbol{s}_h\|_\infty \le C_\infty\|\nabla\boldsymbol{u}\|_\infty, \tag{14}$$

Alson what follows, $\Pi_h^{\rm div} : L^2(\Omega)^d \to V_h^{\rm div}$ will denote the so-called discrete Leray projection, which is the orthogonal projection of $L^2(\Omega)^d$ onto $V_h^{\rm div}$

$$\left(\Pi_h^{\rm div}\boldsymbol{v}, \boldsymbol{w}_h\right) = (\boldsymbol{v}, \boldsymbol{w}_h) \quad \forall \boldsymbol{w}_h \in V_h^{\rm div}.$$

By definition, it is clear that the projection is stable in the $L^2(\Omega)^d$ norm: $\|\Pi_h^{\rm div}\boldsymbol{v}\|_0 \leq \|\boldsymbol{v}\|_0$ for all $\boldsymbol{v} \in L^2(\Omega)^d$. The following well-known bound will be used

$$\|(I - \Pi_h^{\rm div})\boldsymbol{v}\|_0 + h\|(I - \Pi_h^{\rm div})\boldsymbol{v}\|_1 \leq Ch^{j+1}\|\boldsymbol{v}\|_{j+1} \quad \forall \boldsymbol{v} \in V^{\rm div} \cap H^{j+1}(\Omega)^d,$$

for $j = 0, \ldots, k$. This bound follows from the inverse inequality (4), (11) and from the fact $\|(I - \Pi_h^{\rm div})\boldsymbol{v}\|_0 \leq \|\boldsymbol{v} - \boldsymbol{w}_h\|_0$ for any $\boldsymbol{w}_h \in V_h^{\rm div}$ and, in particular $\|(I - \Pi_h^{\rm div})\boldsymbol{v}\|_0 \leq \|\boldsymbol{v} - \boldsymbol{v}_h\|_0$, where $\boldsymbol{v}_h \in V_h^{\rm div}$ solves the problem $(\nabla \boldsymbol{v}_h, \nabla \boldsymbol{w}_h) = -(\Delta \boldsymbol{v}, \boldsymbol{w}_h)$, for all $\boldsymbol{w}_h \in V_h^{\rm div}$ (i.e., for some $q_h \in Q_h$, the pair $(\boldsymbol{v}_h, q_h)$ is the mixed finite-element approximation to problem (7) with $\nu = 1$ and $\boldsymbol{g} = -\Delta \boldsymbol{v}$).

The method that will be studied for the approximation of the solution of the Navier–Stokes equations (1) is obtained by adding to the Galerkin equations a control of the divergence constraint (grad-div stabilization). More precisely, the following grad-div method will be considered: Find $(\boldsymbol{u}_h, p_h) : (0, T] \to V_h \times Q_h$ such that

$$\begin{aligned}(\partial_t \boldsymbol{u}_h, \boldsymbol{v}_h) + \nu(\nabla \boldsymbol{u}_h, \nabla \boldsymbol{v}_h) + b(\boldsymbol{u}_h, \boldsymbol{u}_h, \boldsymbol{v}_h) - (p_h, \nabla \cdot \boldsymbol{v}_h,)& \\ + (\nabla \cdot \boldsymbol{u}_h, q_h) + \mu(\nabla \cdot \boldsymbol{u}_h, \nabla \cdot \boldsymbol{v}_h) = (\boldsymbol{f}, \boldsymbol{v}_h),&\end{aligned} \tag{15}$$

for all $(\boldsymbol{v}_h, q_h) \in V_h \times Q_h$, with $\boldsymbol{u}_h(0) = I_h \boldsymbol{u}_0$. Here, and in the rest of the paper,

$$b(\boldsymbol{u}, \boldsymbol{v}, \boldsymbol{w}) = (B(\boldsymbol{u}, \boldsymbol{v}), \boldsymbol{w}) \quad \forall \boldsymbol{u}, \boldsymbol{v}, \boldsymbol{w} \in H_0^1(\Omega)^d,$$

where,

$$B(\boldsymbol{u}, \boldsymbol{v}) = (\boldsymbol{u} \cdot \nabla)\boldsymbol{v} + \frac{1}{2}(\nabla \cdot \boldsymbol{u})\boldsymbol{v} \quad \forall \boldsymbol{u}, \boldsymbol{v} \in H_0^1(\Omega)^d.$$

Notice the well-known property

$$b(\boldsymbol{u}, \boldsymbol{v}, \boldsymbol{w}) = -b(\boldsymbol{u}, \boldsymbol{w}, \boldsymbol{v}) \quad \forall \boldsymbol{u}, \boldsymbol{v}, \boldsymbol{w} \in V, \tag{16}$$

such that, in particular, $b(\boldsymbol{u}, \boldsymbol{w}, \boldsymbol{w}) = 0$ for all $\boldsymbol{u}, \boldsymbol{w} \in V$. Property (16) in combination with the grad-div term plays a crucial role in our error analysis in order to obtain error constants that do not depend on inverse powers of ν. Whether this is possible with other forms of the nonlinear term (see e. g., [15]) do not seem to have a straightforward answer and will be subject of further studies.

3 Euler incremental projection method

In this section we get error bounds for the grad-div approximations to the Navier-Stokes equations and the Euler incremental projection method. For the Euler incremental scheme the analysis of the semidiscretization in time can be found in [42]. The Euler incremental scheme with a spatial discretization based on inf-sup stable mixed finite elements is analyzed in [33]. Our aim is to get error bounds with constants independent on inverse powers of the viscosity parameter (apart from the dependence through norms of the theoretical solution). For this reason we add grad-div stabilization to the plain Galerkin approximations. For the error analysis we follow both the bounds in [33] for the analysis of the projection scheme and the techniques in [26] for getting bounds independent on the inverse of the viscosity. We will consider a uniform partition of the time interval $[0,T]$ with step-size Δt.

Let $\tilde{\boldsymbol{u}}_h^n \in V_h$, $\boldsymbol{u}_h^n \in V_h + \nabla Q_h$, $p_h^n \in Q_h$ be defined by

$$\left(\frac{\tilde{\boldsymbol{u}}_h^{n+1} - \boldsymbol{u}_h^n}{\Delta t}, \boldsymbol{v}_h\right) + \nu(\nabla \tilde{\boldsymbol{u}}_h^{n+1}, \nabla \boldsymbol{v}_h) + (B(\tilde{\boldsymbol{u}}_h^n, \tilde{\boldsymbol{u}}_h^{n+1}), \boldsymbol{v}_h) - (p_h^n, \nabla \cdot \boldsymbol{v}_h)$$
$$+\mu(\nabla \cdot \tilde{\boldsymbol{u}}_h^{n+1}, \nabla \cdot \boldsymbol{v}_h) = (\boldsymbol{f}^{n+1}, \boldsymbol{v}_h), \quad \forall \boldsymbol{v}_h \in V_h, \tag{17}$$
$$(\nabla \cdot \tilde{\boldsymbol{u}}_h^{n+1}, q_h) = -\Delta t(\nabla(p_h^{n+1} - p_h^n), \nabla q_h), \quad \forall q_h \in Q_h, \tag{18}$$
$$\boldsymbol{u}_h^{n+1} = \tilde{\boldsymbol{u}}_h^{n+1} - \Delta t \nabla(p_h^{n+1} - p_h^n). \tag{19}$$

Let us observe that from (19)

$$(\boldsymbol{u}_h^{n+1}, \nabla q_h) = (\tilde{\boldsymbol{u}}_h^{n+1}, \nabla q_h) - \Delta t(\nabla(p_h^{n+1} - p_h^n), \nabla q_h), \quad \forall q_h \in Q_h,$$

and then applying (18) we get

$$(\boldsymbol{u}_h^{n+1}, \nabla q_h) = 0, \quad \forall q_h \in Q_h. \tag{20}$$

As pointed out in the introduction, the value of the stabilization parameter μ depends on the physical units and there is no clear-cut choice for it.

Let us also observe that since $V_h \subset V$ then $\tilde{\boldsymbol{u}}_h^n \in V_h$ satisfies the homogeneous Dirichlet boundary conditions of the problem. Also, we notice that using (19) in (17) we can express the method in terms of $\tilde{\boldsymbol{u}}_h^n$ as

$$\left(\frac{\tilde{\boldsymbol{u}}_h^{n+1} - \tilde{\boldsymbol{u}}_h^n}{\Delta t}, \boldsymbol{v}_h\right) + \nu(\nabla \tilde{\boldsymbol{u}}_h^{n+1}, \nabla \boldsymbol{v}_h) + (B(\tilde{\boldsymbol{u}}_h^n, \tilde{\boldsymbol{u}}_h^{n+1}), \boldsymbol{v}_h) - (2p_h^n - p_h^{n-1}, \nabla \cdot \boldsymbol{v}_h)$$
$$+ \mu(\nabla \cdot \tilde{\boldsymbol{u}}_h^{n+1}, \nabla \cdot \boldsymbol{v}_h) = (\boldsymbol{f}^{n+1}, \boldsymbol{v}_h), \quad \forall \boldsymbol{v}_h \in V_h,$$

Let us observe that, following [33], we have an implicit-explicit scheme where the linear viscosity term is implicit and a semi-implicit treatment of the non-linear term is considered. Clearly, the semi-implicit treatment of the non-linear term can be easily implemented compared with the fully-implicit treatment of the non-linear term while, as it will be proved in the analysis, the method does not lose the optimal rate of convergence in time. Although other choices are possible, for example, $B(2\tilde{\boldsymbol{u}}_h^n - \tilde{\boldsymbol{u}}_h^{n-1}, \tilde{\boldsymbol{u}}_h^{n+1})$ in (17), for the analysis and for simplicity we choose the simplest form in (17) for which we do not lose the optimal rate of convergence in time. In any case, the reader will find no difficulty in adapting the proofs of the present paper to other kind of extrapolations from previous time steps used frequently in the literature.

In what follows we will denote by

$$\tilde{\boldsymbol{e}}_h^n = \tilde{\boldsymbol{u}}_h^n - \boldsymbol{s}_h^n, \quad \boldsymbol{e}_h^n = \boldsymbol{u}_h^n - \boldsymbol{s}_h^n, \quad \psi_h^n = \pi_h p^{n+1} - p_h^n, \quad \epsilon_h^n = p_h^n - \pi_h p^n.$$

Arguing as in [33] it is easy to get the error equations

$$\left(\frac{\tilde{\boldsymbol{e}}_h^{n+1}-\tilde{\boldsymbol{e}}_h^n}{\Delta t},\boldsymbol{v}_h\right)+\nu(\nabla\tilde{\boldsymbol{e}}_h^{n+1},\nabla\boldsymbol{v}_h)+(B(\tilde{\boldsymbol{u}}_h^n,\tilde{\boldsymbol{u}}_h^{n+1})-B(\boldsymbol{s}_h^n,\boldsymbol{s}_h^{n+1}),\boldsymbol{v}_h)$$
$$+\mu(\nabla\cdot\tilde{\boldsymbol{e}}_h^{n+1},\nabla\cdot\boldsymbol{v}_h)-(2\epsilon_h^n-\epsilon_h^{n-1},\nabla\cdot\boldsymbol{v}_h)$$
$$=(\tau_{1,h}^{n+1},\boldsymbol{v}_h)+(\tau_{2,h}^{n+1},\boldsymbol{v}_h)+(\tau_{3,h}^{n+1},\nabla\cdot\boldsymbol{v}_h)+(\tau_{4,h}^{n+1},\nabla\cdot\boldsymbol{v}_h),\quad\forall\boldsymbol{v}_h\in V_h,\tag{21}$$
$$(\nabla\cdot\tilde{\boldsymbol{e}}_h^{n+1},q_h)+\Delta t(\nabla(\epsilon_h^{n+1}-\epsilon_h^n),\nabla q_h)=\Delta t(\nabla\tau_{5,h}^{n+1},\nabla q_h),\quad\forall q_h\in Q_h.\tag{22}$$

where

$$\tau_{1,h}^{n+1}=\boldsymbol{u}_t^{n+1}-\frac{\boldsymbol{s}_h^{n+1}-\boldsymbol{s}_h^n}{\Delta t},\quad\tau_{2,h}^{n+1}=B(\boldsymbol{u}^{n+1},\boldsymbol{u}^{n+1})-B(\boldsymbol{s}_h^n,\boldsymbol{s}_h^{n+1}),$$
$$\tau_{3,h}^{n+1}=-l_h^{n+1}+\pi_h(2p^n-p^{n-1})-p^{n+1},\quad\tau_{4,h}^{n+1}=\mu\nabla\cdot(\boldsymbol{u}^{n+1}-\boldsymbol{s}_h^{n+1}),$$
$$\tau_{5,h}^{n+1}=-\pi_h(p^{n+1}-p^n).$$

Let us also observe that from (19) it follows that

$$\boldsymbol{e}_h^n=\tilde{\boldsymbol{e}}_h^n-\Delta t\nabla(\epsilon_h^n-\epsilon_h^{n-1})+\Delta t\nabla\tau_{5,h}^n.\tag{23}$$

3.1 Error bounds for the velocity

The error estimates that we obtain in this section depend on the following constants

$$L_1=C_\infty\max_{0\le t\le T}\|\nabla\boldsymbol{u}(t)\|_\infty,\quad L_2=C_\infty\max_{0\le t\le T}\|\boldsymbol{u}(t)\|_2,\tag{24}$$

where C_∞ is the constant in (14),

$$C_0=C_B\max_{0\le t\le 0}\big(\|\boldsymbol{u}(t)\|_\infty^2+\|\boldsymbol{u}(t)\|_2^2\big),\tag{25}$$

where C_B is the constant in (40) below,

$$C_1=CT\Big(\big(C_0C_{\boldsymbol{s}}+\mu+\frac{1}{\mu}\big)\max_{0\le t\le T}\|\boldsymbol{u}(t)\|_{k+1}^2+\frac{1}{\mu}\max_{0\le t\le T}\|p(t)\|_k^2\Big)$$
$$+C\int_0^T\|\boldsymbol{u}_t(t)\|_k^2\,dt,\tag{26}$$
$$C_2=C\int_0^T\big(\|\boldsymbol{u}_{tt}(t)\|_0^2\,dt+C_0\|\nabla\boldsymbol{u}_t(t)\|_0^2+\|\nabla p_t(t)\|_0^2\big)\,dt\tag{27}$$
$$C_3=C\frac{1}{\mu}\int_0^T\|p_{tt}(t)\|_0^2,\tag{28}$$

C_0 being the constant in (25) and C a generic constant depending on Ω and the generic constants in Section 2.

We now state the key result in obtaining the error bounds. Its proof will be given at the end of the section as a consequence of some previous lemmas.

Proposition 1 *Let $\hat{L}$ denote $\hat{L} = 1 + 4(L_1 + L_2^2/\mu)$. The following bound holds for $h \leq 1$, $\Delta t \leq 1/\hat{L}$ and $0 \leq t_n \leq T$:*

$$\|\tilde{\boldsymbol{e}}_h^n\|_0^2 + (\Delta t)^2 \|\nabla \epsilon_h^n\|_0^2 + \Delta t \sum_{j=1}^{n} \big(2\nu \|\nabla \tilde{\boldsymbol{e}}_h^j\|_0^2 + \mu \|\nabla \cdot \tilde{\boldsymbol{e}}_h^j\|_0^2\big) \tag{29}$$
$$\leq e^{n\hat{L}\Delta t} \left(\|\tilde{\boldsymbol{e}}_h^0\|_0^2 + \Delta t \frac{\mu}{2} \|\nabla \cdot \tilde{\boldsymbol{e}}_h^0\|_0^2 + (\Delta t)^2 \|\nabla \epsilon_h^0\|_0^2 + C_1 h^{2k} + C_2 (\Delta t)^2 + C_3 (\Delta t)^4 \right).$$

Remark 2 Let us also observe that adding $\pm \boldsymbol{s}_h^{n+1}$ to (19) we have

$$\boldsymbol{e}_h^{n+1} = \tilde{\boldsymbol{e}}_h^{n+1} - \Delta t \nabla (p_h^{n+1} - p_h^n), \tag{30}$$

so that taking the inner product with $\boldsymbol{e}_h^{n+1}$ and recalling the orthogonality condition (20) we get

$$\|\boldsymbol{e}_h^{n+1}\|_0^2 - \|\tilde{\boldsymbol{e}}_h^{n+1}\|_0^2 + \|\tilde{\boldsymbol{e}}_h^{n+1} - \boldsymbol{e}_h^{n+1}\|_0^2 = 0.$$

Then, $\|\boldsymbol{e}_h^{n+1}\|_0 \leq \|\tilde{\boldsymbol{e}}_h^{n+1}\|_0$ and any estimate of $\|\tilde{\boldsymbol{e}}_h^{n+1}\|_0$ also holds for $\|\boldsymbol{e}_h^{n+1}\|_0$.

To obtain the above error bounds, we will use the following discrete Gronwall lemma that can be found in [34].

Lemma 1 *Let k, B, and a_n, b_n, c_n, γ_n be nonnegative numbers such that*

$$a_n + k \sum_{j=0}^{n} b_j \leq k \sum_{j=0}^{n} \gamma_n a_j + k \sum_{j=0}^{n} c_j + B, \quad n \geq 1.$$

Suppose that $k\gamma_n < 1$, for all n, and set $\sigma_n = (1 - k\gamma_n)^{-1}$. Then, the following bound holds

$$a_n + k \sum_{j=0}^{n} b_j \leq \exp\left(k \sum_{j=0}^{n} \sigma_j \gamma_j \right) \left(k \sum_{j=0}^{n} c_j + B \right), \quad n \geq 1.$$

The convergence result in Theorem 1 will be obtained using stability plus consistency arguments. The following Lemma shows stability. It has two statements. The second one (35) will follow easily after proving the first one (33), which is the stability for linear problems.

Lemma 2 *Let $(\boldsymbol{w}_h^n)_{n=0}^{\infty}$ and $(\boldsymbol{b}_h^n)_{n=1}^{\infty}$ sequences in V_h and $(y_h^n)_{n=0}^{\infty}$ a sequence in Q_h and $(r^n)_{n=1}^{\infty}$ and $(d^n)_{n=1}^{\infty}$ sequences in $H^1(\Omega)$ and $L^2(\Omega)$, respectively, satisfying for all $\boldsymbol{\chi}_h \in V_h$ and $\phi_h \in Q_h$*

$$\left(\frac{\boldsymbol{w}_h^{n+1} - \boldsymbol{w}_h^n}{\Delta t}, \boldsymbol{\chi}_h \right) + \nu (\nabla \boldsymbol{w}_h^{n+1}, \nabla \boldsymbol{\chi}_h) + \mu (\nabla \cdot \boldsymbol{w}_h^{n+1}, \nabla \cdot \boldsymbol{\chi}_h)$$
$$- (2y_h^n - y_h^{n-1}, \nabla \cdot \boldsymbol{\chi}_h) = (\boldsymbol{b}_h^{n+1}, \boldsymbol{\chi}_h) + (d^{n+1}, \nabla \cdot \boldsymbol{\chi}_h), \tag{31}$$
$$(\nabla \cdot \boldsymbol{w}_h^{n+1}, \phi_h) + \Delta t (\nabla (y_h^{n+1} - y_h^n), \nabla \phi_h) = \Delta t (\nabla r^{n+1}, \nabla \phi_h), \tag{32}$$

where $y_h^{-1} = y_h^0$. *Assume that* $0 < \Delta t \le 1$ *Then, for* $n \ge 1$ *the following bound holds,*

$$\begin{aligned}
\|\boldsymbol{w}_h^n\|_0^2 + &(\Delta t)^2\|\nabla y_h^n\|_0^2 + \Delta t\sum_{j=1}^n\bigl(2\nu\|\nabla \boldsymbol{w}_h^j\|_0^2 + \mu\|\nabla\cdot\boldsymbol{w}_h^j\|_0^2\bigr)\\
&\le e^{nL\Delta t}\Biggl(\|\boldsymbol{w}_h^0\|_0^2 + (\Delta t)^2\|\nabla y_h^0\|_0^2 \qquad (33)\\
&\qquad + \Delta t\sum_{j=1}^n\Bigl(4\|\boldsymbol{b}_h^j\|_0^2 + \frac{1}{\mu}\|d^j\|_0^2 + 52\|\nabla r^j\|_0^2 + 33\|\nabla r^{j-1}\|_0^2\Bigr)\Biggr),
\end{aligned}$$

where $L = 1$. *Furthermore, if, on the right-hand side of* (21), $\boldsymbol{b}_h^{n+1}$ *is replaced by* $\boldsymbol{b}_h^{n+1} + \boldsymbol{g}^n(\boldsymbol{w}_h^n, \boldsymbol{w}_h^{n+1})$, *where* $\boldsymbol{g}^n : V_h \times V_h \to L^2(\Omega)^d$ *satisfies that for some* $L_1, L_2 > 0$

$$|(\boldsymbol{g}^n(\boldsymbol{y}_h, \boldsymbol{v}_h), \boldsymbol{v}_h)| \le L_1\|\boldsymbol{y}_h\|_0\|\boldsymbol{v}_h\|_0 + L_2\|\nabla\cdot\boldsymbol{y}_h\|_0\|\boldsymbol{v}_h\|_0, \qquad n \ge 0, \qquad (34)$$

holds for all $\boldsymbol{y}_h, \boldsymbol{v}_h \in V_h$, *then, the following bound holds*

$$\begin{aligned}
\|\boldsymbol{w}_h^n\|_0^2 + &(\Delta t)^2\|\nabla y_h^n\|_0^2 + \Delta t\sum_{j=1}^n\bigl(2\nu\|\nabla \boldsymbol{w}_h^j\|_0^2 + \mu\|\nabla\cdot\boldsymbol{w}_h^j\|_0^2\bigr)\\
&\le e^{n\hat{L}\Delta t}\Biggl(\|\boldsymbol{w}_h^0\|_0^2 + \frac{\mu}{2}\Delta t\|\nabla\cdot\boldsymbol{w}_h^0\|_0^2 + (\Delta t)^2\|\nabla y_h^0\|_0^2 \qquad (35)\\
&\qquad + \Delta t\sum_{j=1}^n\Bigl(4\|\boldsymbol{b}_h^j\|_0^2 + \frac{2}{\mu}\|d^j\|_0^2 + 52\|\nabla r^j\|_0^2 + 33\|\nabla r^{j-1}\|_0^2\Bigr)\Biggr),
\end{aligned}$$

where $\hat{L} = 1 + 4(L_1 + L_2^2/\mu)$.

The proof of the Lemma can be found in the Appendix.

The estimation of the truncation errors (except that of $\tau_{2,h}$) is given in the following result

Lemma 3 *The truncation errors satisfy the following bounds:*

$$\|\tau_{1,h}^n\|_0^2 \le C\frac{h^{2k}}{\Delta t}\int_{t_{n-1}}^{t_n}\|\boldsymbol{u}_t(t)\|_k^2\,dt + C\Delta t\int_{t_{n-1}}^{t_n}\|\boldsymbol{u}_{tt}\|_0^2\,dt, \qquad (36)$$

$$\|\tau_{3,h}^n\|_0^2 \le Ch^{2k}\Bigl(\max_{0\le t\le T}\|\boldsymbol{u}\|_{k+1}^2 + \max_{0\le t\le T}\|p(t)\|_k^2\Bigr) + (\Delta t)^3\int_{t_{n-1}}^{t_{n+1}}\|p_{tt}\|_0^2\,dt, \qquad (37)$$

$$\|\tau_{4,h}^n\|_0^2 \le C\mu^2h^{2k}\|\boldsymbol{u}^n\|_{k+1}^2, \qquad (38)$$

$$\|\nabla\tau_{h,5}^n\|_0^2 \le C\Delta t\int_{t_{n-1}}^{t_n}\|\nabla p_t\|_0^2\,dt. \qquad (39)$$

Proof For the first one we have

$$\begin{aligned}
\tau_{1,h}^n &= \frac{(\boldsymbol{u}^n - \boldsymbol{s}_h^n) - (\boldsymbol{u}^{n-1} - \boldsymbol{s}_h^{n-1})}{\Delta t} + \Bigl(\boldsymbol{u}_t^n - \frac{\boldsymbol{u}^n - \boldsymbol{u}^{n-1}}{\Delta t}\Bigr)\\
&= \frac{1}{\Delta t}\int_{t_{n-1}}^{t_n}(\boldsymbol{u} - \boldsymbol{s}_h)_t(t)\,dt + \frac{1}{\Delta t}\int_{t_{n-1}}^{t_n}(t - t_{n-1})\boldsymbol{u}_{tt}(t)\,dt.
\end{aligned}$$

Applying (11) and Cauchy-Schwarz the first estimate (36) follows.

To estimate $\tau_{3,h}$ we write

$$\pi_h(2p^n - p^{n-1}) - p^{n+1} = (\pi_h - I)(2p^n - p^{n-1}) + 2p^n - p^{n-1} - p^{n+1}.$$

By writing

$$\begin{aligned} 2p^n - p^{n-1} - p^{n+1} &= -\big((p^{n+1} - p^n) - (p^n - p_{n-1})\big) = -\int_{t_n}^{t_{n+1}} p_t\,dt + \int_{t_{n-1}}^{t_n} p_t\,dt \\ &= -\int_{t_n-\Delta t/2}^{t_n+\Delta t/2} \left(\int_{t-\Delta t/2}^{t+\Delta t/2} p_{ss}\,ds\right) dt. \end{aligned}$$

and applying (12), (5) and Hölder's inequality one obtains the estimate (37).

The bound $\tau_{4,h}$ is a direct consequence of (11). Finally, for $\tau_{h,5}$ we may write, using the H^1 stability of the projection π_h,

$$\|\nabla \tau_{h,5}^n\|^2 = \|\nabla \pi_h(p^n - p^{n-1})\|_0^2 \le C\|\nabla(p^n - p^{n-1})\|_0^2 = C\left\|\int_{t_{n-1}}^{t_n} \nabla p_t\,dt\right\|_0^2,$$

so that applying Hölder's inequality the estimate (39) follows □

To bound the truncation error $\tau_{2,h}$ we will apply the following lemma.

Lemma 4 *There exists a positive constant C_B such that the following bound holds*

$$\begin{aligned} &\|B(\boldsymbol{u}^{n+1}, \boldsymbol{u}^{n+1}) - B(\boldsymbol{s}_h^n, \boldsymbol{s}_h^{n+1})\|_0 \\ &\quad \le C_B\big(\|\boldsymbol{u}\|_{L^\infty(L^\infty(\Omega)^d)} + \|\boldsymbol{u}\|_{L^\infty(H^2(\Omega)^d)}\big)\Big(\|\boldsymbol{u}^n - \boldsymbol{s}_h^n\|_1 + \|\boldsymbol{u}^{n+1} - \boldsymbol{s}_h^{n+1}\|_1 \\ &\qquad + (\Delta t)^{1/2}\big(\int_{t_n}^{t_{n+1}} \|\nabla \boldsymbol{u}_t\|_0^2\,dt\big)^{1/2}\Big) \end{aligned} \tag{40}$$

Proof We decompose

$$\begin{aligned} \|B(\boldsymbol{u}^{n+1}, \boldsymbol{u}^{n+1}) - B(\boldsymbol{s}_h^n, \boldsymbol{s}_h^{n+1})\|_0 \le &\|B(\boldsymbol{u}^{n+1} - \boldsymbol{u}^n, \boldsymbol{u}^{n+1})\|_0 + \|B(\boldsymbol{u}^n - \boldsymbol{s}_h^n, \boldsymbol{s}_h^{n+1})\|_0 \\ &+ \|B(\boldsymbol{u}^n, \boldsymbol{u}^{n+1} - \boldsymbol{s}_h^{n+1})\|_0. \end{aligned}$$

For the first term on the right-hand side above applying (2) we write

$$\begin{aligned} \|B(\boldsymbol{u}^{n+1} - \boldsymbol{u}^n, \boldsymbol{u}^{n+1})\|_0 &= \|(\boldsymbol{u}^{n+1} - \boldsymbol{u}^n)\cdot\nabla\boldsymbol{u}\|_0 \le \|\boldsymbol{u}^{n+1} - \boldsymbol{u}^n\|_{L^{2d}}\|\nabla\boldsymbol{u}^{n+1}\|_{L^{2d/(d-1)}} \\ &\le C\|\boldsymbol{u}\|_{L^\infty(H^2(\Omega)^d)}\|\nabla(\boldsymbol{u}^{n+1} - \boldsymbol{u}^n)\|_0 \\ &\le C\|\boldsymbol{u}\|_{L^\infty(H^2(\Omega)^d)}(\Delta t)^{1/2}\left(\int_{t_n}^{t_{n+1}} \|\nabla\boldsymbol{u}_t\|_0^2\,dt\right)^{1/2}. \end{aligned}$$

For the other two terms arguing similarly we get

$$\begin{aligned} \|B(\boldsymbol{u}^n - \boldsymbol{s}_h^n, \boldsymbol{s}_h^{n+1})\|_0 + \|B(\boldsymbol{u}^n, \boldsymbol{u}^{n+1} - \boldsymbol{s}_h^{n+1})\|_0 &\le \|\boldsymbol{u}^n - \boldsymbol{s}_h^n\|_{L^{2d}}\|\nabla\boldsymbol{s}_h^{n+1}\|_{L^{2d/(d-1)}} \\ &\quad + \frac{1}{2}\|\nabla\cdot(\boldsymbol{u}^n - \boldsymbol{s}_h^n)\|_0\|\boldsymbol{s}_h^{n+1}\|_\infty + \|\boldsymbol{u}^n\|_\infty\|\boldsymbol{u}^{n+1} - \boldsymbol{s}_h^{n+1}\|_1 \\ \le C\left(\|\nabla\boldsymbol{s}_h^{n+1}\|_{L^{2d/(d-1)}} + \|\boldsymbol{s}_h^{n+1}\|_\infty + \|\boldsymbol{u}^n\|_\infty\right)&\left(\|\boldsymbol{u}^n - \boldsymbol{s}_h^n\|_1 + \|\boldsymbol{u}^{n+1} - \boldsymbol{s}_h^{n+1}\|_1\right) \end{aligned}$$

Recall that $\|\boldsymbol{s}_h^{n+1}\|_\infty$ has ben estimated in (14). To estimate $\|\nabla \boldsymbol{s}_h^{n+1}\|_{L^{2d/(d-1)}}$ we write

$$\nabla \boldsymbol{s}_h^{n+1} = \nabla(\boldsymbol{s}_h^{n+1} - I_h(\boldsymbol{u}^{n+1})) + \nabla(I_h(\boldsymbol{u}^{n+1}) - \boldsymbol{u}^{n+1}) + \nabla \boldsymbol{u}^{n+1},$$

so that applying (4), (11), and (6) we have

$$\|\nabla(\boldsymbol{s}_h^{n+1} - I_h(\boldsymbol{u}^{n+1}))\|_{L^{2d/(d-1)}} \le Ch^{-1/2}\|\nabla(\boldsymbol{s}_h^{n+1} - \boldsymbol{u}^{n+1})\|_0 \le Ch^{1/2}\|\boldsymbol{u}^{n+1}\|_2$$
$$\|\nabla(I_h(\boldsymbol{u}^{n+1}) - \boldsymbol{u}^{n+1})\|_{L^{2d/(d-1)}} \le Ch^{1/2}\|\boldsymbol{u}^{n+1}\|_2,$$

and then, applying also Sobolev's inequality (2) if follows that

$$\|\nabla \boldsymbol{s}_h^{n+1}\|_{L^{2d/(d-1)}} \le Ch^{1/2}\|\boldsymbol{u}^{n+1}\|_2 + \|\nabla \boldsymbol{u}^{n+1}\|_{L^{2d/(d-1)}} \le C(h^{1/2}+1)\|\boldsymbol{u}^{n+1}\|_2. \quad (41)$$

and the conclusion is reached. □

Applying Lemma 4 and (11) we get

$$\begin{aligned}\|\tau_{2,h}^n\|_0^2 &\le C_B\big(\|\boldsymbol{u}\|^2_{L^\infty(L^\infty(\Omega)^d)} + \|\boldsymbol{u}\|^2_{L^\infty(H^2(\Omega)^d)}\big)\Big(\|\boldsymbol{u}^n - \boldsymbol{s}_h^n\|_1^2 + \|\boldsymbol{u}^{n-1} - \boldsymbol{s}_h^{n-1}\|_1^2 \\ &\qquad + \Delta t \int_{t_{n-1}}^{t_n} \|\nabla \boldsymbol{u}_t\|_0^2 \, dt\Big) \\ &\le C_0\bigg(C_{\boldsymbol{s}} h^{2k}(\|\boldsymbol{u}^n\|^2_{k+1} + \|\boldsymbol{u}^{n-1}\|^2_{k+1}) + \Delta t \int_{t_{n-1}}^{t_n} \|\nabla \boldsymbol{u}_t\|_0^2 \, dt\bigg). \end{aligned} \quad (42)$$

where $C_{\boldsymbol{s}}$ and C_0 are the constants in (11) and (25), respectively.

Proof of Proposition 1. We will apply Lemma 2 to the error equations (21–22), that is, in Lemma 2 we take $\boldsymbol{w}_h^n = \tilde{\boldsymbol{e}}_h^n$, $y_h^n = \epsilon_h^n$, $\boldsymbol{b}_h^n = \tau_{1,h}^n + \tau_{2,h}^n$, $d_h^n = \tau_{3,h}^n + \tau_{4,h}^n$, $r_h^n = \tau_{h,5}^n$ and

$$\boldsymbol{g}^n(\boldsymbol{y}_h, \boldsymbol{v}_h) = B(\boldsymbol{y}_h, \boldsymbol{s}_h^{n+1}) + B(\tilde{\boldsymbol{u}}_h^n, \boldsymbol{v}_h),$$

since, an easy calculation shows

$$\begin{aligned} B(\tilde{\boldsymbol{u}}_h^n, \tilde{\boldsymbol{u}}_h^{n+1}) - B(\boldsymbol{s}_h^n, \boldsymbol{s}_h^{n+1}) &= B(\tilde{\boldsymbol{e}}_h^n, \boldsymbol{s}_h^{n+1}) + B(\tilde{\boldsymbol{u}}_h^n, \tilde{\boldsymbol{e}}_h^{n+1}) \\ &= \boldsymbol{g}^n(\tilde{\boldsymbol{e}}_h^n, \tilde{\boldsymbol{e}}_h^{n+1}). \end{aligned}$$

Prior to applying Lemma 2 we must check that condition (34) holds. For that purpose, using the skew-symmetric property of the nonlinear term (16), we can write

$$\begin{aligned} (\boldsymbol{g}^n(\boldsymbol{y}_h, \boldsymbol{v}_h), \boldsymbol{v}_h) &= (B(\boldsymbol{y}_h, \boldsymbol{s}_h^{n+1}), \boldsymbol{v}_h) \\ &\le \|\nabla \boldsymbol{s}_h^{n+1}\|_\infty \|\boldsymbol{y}_h\|_0 \|\boldsymbol{v}_h\|_0 + \frac{1}{2}\|\nabla \cdot \boldsymbol{y}_h\|_0 \|\boldsymbol{s}_h^{n+1}\|_\infty \|\boldsymbol{v}_h\|_0. \end{aligned}$$

so that applying the estimates (14) it follows that

$$(\boldsymbol{g}^n(\boldsymbol{y}_h, \boldsymbol{v}_h), \boldsymbol{v}_h) = L_1\|\boldsymbol{y}_h\|_0\|\boldsymbol{v}_h\|_0 + L_2\|\nabla \cdot \boldsymbol{y}_h\|_0\|\boldsymbol{v}_h\|_0,$$

where L_1 and L_2 are the constants in (24). Thus, we can apply (35) to the error equations (21–22). Let us observe that the assumption $y_h^{-1} = y_h^0$ is in our case $\epsilon_h^{-1} = \epsilon_h^0$. This means we take $\tilde{\boldsymbol{u}}_h^0 = \boldsymbol{u}_h^0$ so that equation (22) holds for $n+1=0$ with $\epsilon_h^{-1} = \epsilon_h^0$ and $r_h^0 = \tau_{5,h}^0 = 0$.

Thus, applying (35) to (21–22) and taking into account the estimates (36)–(39) and (42) we conclude the bound (29). □

We now state the main result of this section, whose proof is a direct consequence of the estimate (11), Remark 2 and Proposition 1. For simplicity we set $\boldsymbol{u}_0 = \tilde{\boldsymbol{u}}_0 = \boldsymbol{s}_h(0)$ and $p_h^0 = \pi_h p(0)$, but, in view of Proposition 1, the reader will find no difficulty in proving error bounds corresponding to different initial conditions.

Theorem 1 *Let $\hat{L}$ denote $\hat{L} = 1 + 4(L_1 + L_2^2/\mu)$ and set $\boldsymbol{u}_0 = \tilde{\boldsymbol{u}}_0 = \boldsymbol{s}_h(0)$ and $p_h^0 = \pi_h p(0)$. Then, the following bound holds for $h \le 1$, $\Delta t \le 1/\hat{L}$ and $0 \le t_n \le T$:*

$$\|\boldsymbol{u}_h^n - \boldsymbol{u}(t_n)\|_0^2 + \|\tilde{\boldsymbol{u}}_h^n - \boldsymbol{u}(t_n)\|_0^2 + \Delta t \sum_{j=1}^n \mu \|\nabla \cdot \tilde{\boldsymbol{u}}_h^n\|_0^2 \\ \le 2\left(C_{\boldsymbol{s}}^2(2+\mu T) + e^{\hat{L}T}\right)C_1 h^{2k} + 2e^{\hat{L}T}\left(C_2(\Delta t)^2 + C_3(\Delta t)^4\right).$$

3.2 Error bounds for the pressure

Observe that from (23) we get

$$\frac{\boldsymbol{e}_h^{n+1} - \boldsymbol{e}_h^n}{\Delta t} - \frac{\tilde{\boldsymbol{e}}_h^{n+1} - \tilde{\boldsymbol{e}}_h^n}{\Delta t} = -\nabla(\epsilon_h^{n+1} - 2\epsilon_h^n + \epsilon_h^{n-1}) + \nabla(\tau_{5,h}^{n+1} - \tau_{5,h}^n)$$

so that adding this equality to (21) we have

$$\left(\frac{\boldsymbol{e}_h^{n+1} - \boldsymbol{e}_h^n}{\Delta t}, \boldsymbol{v}_h\right) + \nu(\nabla \tilde{\boldsymbol{e}}_h^{n+1}, \nabla \boldsymbol{v}_h) + (B(\tilde{\boldsymbol{u}}_h^n, \tilde{\boldsymbol{u}}_h^{n+1}) - B(\boldsymbol{s}_h^n, \boldsymbol{s}_h^{n+1}), \boldsymbol{v}_h) \\ +\mu(\nabla \cdot \tilde{\boldsymbol{e}}_h^{n+1}, \nabla \cdot \boldsymbol{v}_h) - (\epsilon_h^{n+1}, \nabla \cdot \boldsymbol{v}_h) = \\ (\tau_{1,h}^{n+1}, \boldsymbol{v}_h) + (\tau_{2,h}^{n+1}, \boldsymbol{v}_h) + (\hat{\tau}_{3,h}^{n+1}, \nabla \cdot \boldsymbol{v}_h) + (\tau_{4,h}^{n+1}, \nabla \cdot \boldsymbol{v}_h), \quad \forall \boldsymbol{v}_h \in V_h, \qquad (43)$$

where $\hat{\tau}_{3,h}^{n+1} = -l_h^{n+1} + (\pi_h - I)p^{n+1}$, which, applying (5) and (12) can be bounded as

$$\|\hat{\tau}_{3,h}^n\|_0^2 \le C \max_{0 \le t \le T} h^{2k} \|\boldsymbol{u}\|_{k+1}^2 + Ch^{2k} \max_{0 \le t \le T} \|p(t)\|_k^2. \qquad (44)$$

The error ϵ_h^{n+1} will be estimated by applying the inf-sup condition to (43). This, in turn will require the estimation of a negative norm of $(\boldsymbol{e}_h^{n+1} - \boldsymbol{e}_h^n)/\Delta t$, for which the following result will be needed.

Lemma 5 *Let $\boldsymbol{f} \in L^2$ satisfying*

$$(\boldsymbol{f}, \nabla q_h) = 0, \quad \forall q_h \in Q_h,$$

then the following bound holds

$$\|\boldsymbol{f}\|_{-1} \le C\|(A_h^{\mathrm{div}})^{-1/2}\Pi_h^{\mathrm{div}} \boldsymbol{f}\|_0 + Ch\|\boldsymbol{f}\|_0. \qquad (45)$$

Proof We argue as in [5, Lemma 3.11]. For $\varphi \in H_0^1$ we decompose $\varphi = \Pi\varphi + \nabla\xi$, for some $\xi \in H^2$. Then it holds, (see e.g. [19])

$$\|\Pi\varphi\|_1 \le C\|\varphi\|_1, \quad \|\nabla\xi\|_1 \le C\|\varphi\|_1.$$

Then $(\boldsymbol{f}, \varphi) = (\boldsymbol{f}, \Pi\varphi) + (\boldsymbol{f}, \nabla\xi)$. On the one hand

$$(\boldsymbol{f}, \Pi\varphi) = (\Pi \boldsymbol{f}, \Pi\varphi) = (A^{-1/2}\Pi\boldsymbol{f}, A^{1/2}\Pi\varphi) \le C\|A^{-1/2}\Pi\boldsymbol{f}\|_0\|\varphi\|_1.$$

And, on the other

$$(\boldsymbol{f}, \nabla\xi) = (\boldsymbol{f}, \nabla(\xi - I_{Q_h}\xi)) \le Ch\|\boldsymbol{f}\|_0\|\varphi\|_1,$$

where I_{Q_h} is the standard interpolant in Q_h. Then

$$\|\boldsymbol{f}\|_{-1} \le Ch\|\boldsymbol{f}\|_0 + C\|A^{-1/2}\Pi\boldsymbol{f}\|_0. \tag{46}$$

Finally, to reach (45) we apply [5, (2.15)]

$$\|A^{-1/2}\Pi\boldsymbol{f}\|_0 \le Ch\|\boldsymbol{f}\|_0 + \|(A_h^{\rm div})^{-1/2}\Pi_h^{\rm div}\boldsymbol{f}\|_0, \quad f \in L^2. \tag{47}$$

Inserting (47) into (46) the conclusion is reached. □

Lemma 6 There exist a positive constant C such that the following bound holds:

$$\begin{aligned}\beta_0\|\epsilon_h^{n+1}\|_0 \quad \le \quad & Ch\left\|\frac{\tilde{\boldsymbol{e}}_h^{n+1} - \tilde{\boldsymbol{e}}_h^n}{\Delta t}\right\|_0 + C\nu\|\nabla\tilde{\boldsymbol{e}}_h^{n+1}\|_0 + C\mu\|\nabla\cdot\tilde{\boldsymbol{e}}_h^{n+1}\|_0 \\ & + C\|B(\tilde{\boldsymbol{u}}_h^n, \tilde{\boldsymbol{u}}_h^{n+1}) - B(\boldsymbol{s}_h^n, \boldsymbol{s}_h^{n+1})\|_{-1} \\ & + C\|\tau_{1,h}^{n+1}\|_{-1} + C\|\tau_{2,h}^{n+1}\|_{-1} + C\|\hat{\tau}_{3,h}^{n+1}\|_0 + C\|\tau_{4,h}^{n+1}\|_0.\end{aligned} \tag{48}$$

The proof of the Lemma can be found in the Appendix.

Now, the only term on the right-hand side of (48) whose bound is not standard is the first one. To estimate its value, we will draw ideas from [33]. Let us denote by

$$d_t\boldsymbol{v}^{n+1} = \boldsymbol{v}^{n+1} - \boldsymbol{v}^n.$$

We notice that the first term on the right-hand side of (48) can be written as $\|d_t\tilde{e}_h^n\|_0/\Delta t$. We will estimate its value by applying Lemma 2 to the following set of equations, which can be obtained by subtracting the expressions corresponding to n and $n-1$ (21) and (22):

$$\begin{aligned}&\left(\frac{d_t\tilde{\boldsymbol{e}}_h^{n+1} - d_t\tilde{\boldsymbol{e}}_h^n}{\Delta t}, \boldsymbol{v}_h\right) + \nu(\nabla d_t\tilde{\boldsymbol{e}}_h^{n+1}, \nabla\boldsymbol{v}_h) + (B(\tilde{\boldsymbol{u}}_h^n, \tilde{\boldsymbol{u}}_h^{n+1}) - B(\boldsymbol{s}_h^n, \boldsymbol{s}_h^{n+1}), \boldsymbol{v}_h) \\ &- (B(\tilde{\boldsymbol{u}}_h^{n-1}, \tilde{\boldsymbol{u}}_h^n) - B(\boldsymbol{s}_h^{n-1}, \boldsymbol{s}_h^n), \boldsymbol{v}_h) \\ &+ \mu(\nabla\cdot d_t\tilde{\boldsymbol{e}}_h^{n+1}, \nabla\cdot\boldsymbol{v}_h) + (2d_t(\epsilon_h^n - \epsilon_h^{n-1}), \nabla\cdot\boldsymbol{v}_h) \\ &= (d_t\tau_{1,h}^{n+1}, \boldsymbol{v}_h) + (d_t\tau_{2,h}^{n+1}, \boldsymbol{v}_h) + (d_t\tau_{3,h}^{n+1}, \nabla\cdot\boldsymbol{v}_h) + (d_t\tau_{4,h}^{n+1}, \nabla\cdot\boldsymbol{v}_h), \quad \forall\boldsymbol{v}_h \in V_h,\end{aligned} \tag{49}$$

$$\begin{aligned}(\nabla\cdot d_t\tilde{\boldsymbol{e}}_h^{n+1}, q_h) = -\Delta t(\nabla(d_t\epsilon_h^{n+1} - d_t\epsilon_h^n) \quad , \nabla q_h) + \Delta t(\nabla d_t\tau_{5,h}^{n+1}, \nabla q_h), \\ \forall q_h \in Q_h.\end{aligned} \tag{50}$$

As in Section 3.1, we first estimate the truncation errors.

Lemma 7 *There exists a positive constant C such that the following bound holds*

$$\|d_t\tau_{1,h}^n\|_0^2 \leq C(\Delta t)\Big(h^{2k}\int_{t_{n-2}}^{t_n}\|\boldsymbol{u}_{tt}\|_k^2\,dt + (\Delta t)^2\int_{t_{n-2}}^{t_n}\|\boldsymbol{u}_{ttt}\|_0^2\,dt\Big), \tag{51}$$

$$\|d_t\tau_{3,h}^n\|_0^2 \leq C(\Delta t)h^{2k}\Big(\int_{t_{n-1}}^{t_n}\|\boldsymbol{u}_t\|_{k+1}^2\,dt + \int_{t_{n-2}}^{t_n}\|p_t\|_k^2\,dt\Big) + C(\Delta t)^3\int_{t_{n-3}}^{t_n}\|p_{tt}\|_0^2\,dt, \tag{52}$$

$$\|d_t\tau_{4,h}^n\|_0^2 \leq C(\Delta t)h^{2k}\mu^2\int_{t_{n-1}}^{t_n}\|\boldsymbol{u}_t\|_{k+1}^2,\,dt \tag{53}$$

$$\|d_t\nabla\tau_{h,5}^n\|^2 \leq C(\Delta t)^3\int_{t_{n-2}}^{t_n}\|p_{tt}\|_1^2\,dt. \tag{54}$$

Proof Similarly to the estimation of $\tau_{3,h}^n$ in Lemma 3, we may write

$$d_t\tau_{3,h}^n = \int_{t_{n-1}}^{t_n}\partial_t\Big(l_h(t) + (\pi_h - I)(2p(t) - p(t-\Delta t))\Big)\,dt + \big(2p^{n-1} - p^{n-2} - p^n\big) - \big(2p^{n-2} - p^{n-3} - p^{n-1}\big).$$

The last two terms have already been estimated in (37). For the first one, applying Hölder's inequality, (12) and (5), its L^2 norm can be bounded by

$$(\Delta t)^{1/2}h^k\bigg(C_{\boldsymbol{s}}\Big(\int_{t_{n-1}}^{t_n}\|\boldsymbol{u}_t\|_{k+1}^2\,dt\Big)^{1/2} + C\Big(\int_{t_{n-2}}^{t_n}\|p_t\|_k^2\,dt\Big)^{1/2}\bigg),$$

so that (52) follows easily. With similar arguments the estimate (53) can be otained. For $d_t\tau_{5,h}$ we write

$$\begin{aligned}\|d_t\nabla\tau_{h,5}^{n+1}\|^2 &= \|dt\nabla\pi_h(p^{n+1} - p^n)\|_0^2 \leq C\|\nabla d_t(p^{n+1} - p^n)\|_0^2\\ &= C\|\nabla(p^{n+1} - 2p^n + p^{n-1})\|_0^2,\end{aligned}$$

and the bound is obtained with arguments similar as those used with $\tau_{3,h}$. Finally, for $d_t\tau_{1,h}$ we write

$$d_t\tau_{1,h}^n = \int_{t_{n-1}}^{t_n}\bigg(\frac{(\boldsymbol{u}-\boldsymbol{s}_h)_t(t) - (\boldsymbol{u}-\boldsymbol{s}_h)_t(t-\Delta t)}{\Delta t} + \Big(\boldsymbol{u}_{tt}(t) - \frac{\boldsymbol{u}_t(t) - \boldsymbol{u}_t(t-\Delta t)}{\Delta t}\Big)\bigg)\,dt$$

and the bound (51) is obtained by arguing as in the proof of (36). □

The following result is a direct consequence of the previous lemma.

Lemma 8 *The following bound holds for $n \geq 2$:*

$$\Delta t\sum_{k=2}^n(\|d_t\tau_{1,h}^k\|_0^2 + \|d_t\nabla\tau_{h,5}^k\|_0^2 + \|d_t\nabla\tau_{h,5}^{k-1}\|_0^2) + \frac{1}{\mu}\Delta t\sum_{k=2}^n(\|d_t\tau_{3,h}^k\|_0^2 + \|d_t\tau_{4,h}^k\|_0^2) \leq C(\Delta t)^2(\hat{C}_1h^{2k} + \hat{C}_2(\Delta t)^2),$$

where

$$\hat{C}_1 = \int_0^T \Big(\|\boldsymbol{u}_{tt}\|_k^2 + \Big(\mu + \frac{1}{\mu}\Big) \|\boldsymbol{u}_t\|_{k+1}^2 + \frac{1}{\mu}\|p_t\|_k^2 \Big)\, dt, \tag{55}$$

$$\hat{C}_2 = \int_0^T \Big(\|\boldsymbol{u}_{ttt}\|_0^2 + \|p_{tt}\|_1^2 + \frac{1}{\mu}\|p_{tt}\|_0^2 \Big)\, dt. \tag{56}$$

For the truncation error $d_t\tau_{2,h}$ we have the following result

Lemma 9 *The following bound holds for $n \geq 2$:*

$$\Delta t \sum_{k=2}^{n} (\|d_t \tau_{2,h}^k\|_0^2 \leq C(\Delta t)^2 (\hat{C}_3 h^{2k} + \hat{C}_4 (\Delta t)^2),$$

where

$$\hat{C}_3 = \|\boldsymbol{u}\|_{L^\infty(H^2)}^2 \int_0^T \|\boldsymbol{u}_t\|_{k+1}^2\, dt + \|\boldsymbol{u}\|_{L^\infty(H^{k+1})}^2 \int_0^T \|\boldsymbol{u}_t\|_2^2\, dt, \tag{57}$$

$$\hat{C}_4 = \|\boldsymbol{u}_t\|_{L^\infty(H^1)}^2 \int_0^T \|\boldsymbol{u}_t\|_2^2\, dt + \|\boldsymbol{u}\|_{L^\infty(W^{1,\infty})}^2 \int_0^T \|\boldsymbol{u}_{tt}\|_2^2\, dt. \tag{58}$$

The proof of the Lemma can be found in the Appendix.

In order to apply Lemma 2 to equations (49–50) we need to rewrite the nonlinear terms in (49), $B(\tilde{\boldsymbol{u}}_h^n, \tilde{\boldsymbol{u}}_h^{n+1}) - B(\boldsymbol{s}_h^n, \boldsymbol{s}_h^{n+1}) - (B(\tilde{\boldsymbol{u}}_h^{n-1}, \tilde{\boldsymbol{u}}_h^n) - B(\boldsymbol{s}_h^{n-1}, \boldsymbol{s}_h^n))$. For that purpose, by adding $\pm B(\tilde{\boldsymbol{u}}_h^n, \boldsymbol{s}_h^{n+1})$ and $\pm B(\tilde{\boldsymbol{u}}_h^{n-1}, \boldsymbol{s}_h^n)$ we write

$$\begin{aligned} &B(\tilde{\boldsymbol{u}}_h^n, \tilde{\boldsymbol{u}}_h^{n+1}) - B(\boldsymbol{s}_h^n, \boldsymbol{s}_h^{n+1}) - (B(\tilde{\boldsymbol{u}}_h^{n-1}, \tilde{\boldsymbol{u}}_h^n) - B(\boldsymbol{s}_h^{n-1}, \boldsymbol{s}_h^n)) = \\ &\quad B(\tilde{\boldsymbol{e}}_h^n, \boldsymbol{s}_h^{n+1}) + B(\tilde{\boldsymbol{u}}_h^n, \tilde{\boldsymbol{e}}_h^{n+1}) - (B(\tilde{\boldsymbol{e}}_h^{n-1}, \boldsymbol{s}_h^n) + B(\tilde{\boldsymbol{u}}_h^{n-1}, \tilde{\boldsymbol{e}}_h^n) = \\ &\big(B(\tilde{\boldsymbol{e}}_h^n, \boldsymbol{s}_h^{n+1}) - B(\tilde{\boldsymbol{e}}_h^{n-1}, \boldsymbol{s}_h^n)\big) + \big(B(\tilde{\boldsymbol{u}}_h^n, \tilde{\boldsymbol{e}}_h^{n+1}) - B(\tilde{\boldsymbol{u}}_h^{n-1}, \tilde{\boldsymbol{e}}_h^n)\big). \end{aligned} \tag{59}$$

For the first term on the right-hand side of (59), by adding $\pm B(\tilde{\boldsymbol{e}}_h^n, \boldsymbol{s}_h^n)$ we write

$$B(\tilde{\boldsymbol{e}}_h^n, \boldsymbol{s}_h^{n+1}) - B(\tilde{\boldsymbol{e}}_h^{n-1}, \boldsymbol{s}_h^n) = B(d_t\tilde{\boldsymbol{e}}_h^n, \boldsymbol{s}_h^n) + B(\tilde{\boldsymbol{e}}_h^n, d_t\boldsymbol{s}_h^{n+1}),$$

and, for the second term on the right-hand side of (59), by adding $\pm B(\tilde{\boldsymbol{u}}_h^n, \tilde{\boldsymbol{e}}_h^n)$, and then, $\pm B(d_t\boldsymbol{s}_h^n, \tilde{\boldsymbol{e}}_h^n)$

$$\begin{aligned} B(\tilde{\boldsymbol{u}}_h^n, \tilde{\boldsymbol{e}}_h^{n+1}) - B(\tilde{\boldsymbol{u}}_h^{n-1}, \tilde{\boldsymbol{e}}_h^n) &= B(d_t\tilde{\boldsymbol{u}}_h^n, \tilde{\boldsymbol{e}}_h^n) + B(\tilde{\boldsymbol{u}}_h^n, d_t\tilde{\boldsymbol{e}}_h^{n+1}) \\ &= B(d_t\tilde{\boldsymbol{e}}_h^n, \tilde{\boldsymbol{e}}_h^n) + B(\tilde{\boldsymbol{u}}_h^n, d_t\tilde{\boldsymbol{e}}_h^{n+1}) + B(d_t\boldsymbol{s}_h^n, \tilde{\boldsymbol{e}}_h^n). \end{aligned}$$

Let us denote

$$\boldsymbol{g}^n(\boldsymbol{v}_h, \boldsymbol{w}_h) = B(\boldsymbol{v}_h, \boldsymbol{s}_h^n) + B(\boldsymbol{v}_h, \tilde{\boldsymbol{e}}_h^n) + B(\tilde{\boldsymbol{u}}_h^n, \boldsymbol{w}_h) = B(\boldsymbol{v}_h, \tilde{\boldsymbol{u}}_h^n) + B(\tilde{\boldsymbol{u}}_h^n, \boldsymbol{w}_h) \tag{60}$$

$$\tau_{h,6}^{n+1} = B(\tilde{\boldsymbol{e}}_h^n, d_t\boldsymbol{s}_h^{n+1}) + B(d_t\boldsymbol{s}_h^n, \tilde{\boldsymbol{e}}_h^n),$$

so that the nonlinear terms in (49) can be expressed as

$$\begin{aligned} B(\tilde{\boldsymbol{u}}_h^n, \tilde{\boldsymbol{u}}_h^{n+1}) - B(\boldsymbol{s}_h^n, \boldsymbol{s}_h^{n+1}) - (B(\tilde{\boldsymbol{u}}_h^{n-1}, \tilde{\boldsymbol{u}}_h^n) - B(\boldsymbol{s}_h^{n-1}, \boldsymbol{s}_h^n)) =&\, \boldsymbol{g}^n(d_t\tilde{\boldsymbol{e}}_h^n, d_t\tilde{\boldsymbol{e}}_h^{n+1}) \\ &+ \tau_{h,6}^{n+1}. \end{aligned}$$

Our next step is to show that $\boldsymbol{g}^n$ satisfies the hypothesis of Lemma 2. This will be accomplished with Lemma 10 below. We need to fix some notation first. Let us denote by C_4, L_1' and L_2' the following quantities:

$$C_4 = e^{\hat{L}T/2}(C_1 + C_2 + C_3)^{1/2}. \tag{61}$$

$$L_1' = C(C_4 + \|\boldsymbol{u}\|_{L^\infty(W^{1,\infty}(\Omega)^d)}), \qquad L_2' = C(C_4 + \|\boldsymbol{u}\|_{L^\infty(H^2(\Omega)^d)}). \tag{62}$$

where $\hat{L}$ is that constant in Proposition 1, and C_1, C_2 and C_3 are those defined at the beginning of Section 3.1.

Lemma 10 Assume that $h \le 1$, $\Delta t \le 1$ and that the following condition holds,

$$\Delta t \le C h^{d/2+1}, \quad k \ge d/2 + 1. \tag{63}$$

Then, the functions $\boldsymbol{g}^n$ defined in (60) satisfy the following bound for $n = 2, \dots, N = T/\Delta t$:

$$(\boldsymbol{g}^n(\boldsymbol{v}_h, \boldsymbol{w}_h), \boldsymbol{w}_h) \le L_1' \|\boldsymbol{v}_h^n\|_0 \|\boldsymbol{w}_h\|_0 + L_2' \|\nabla \cdot \boldsymbol{v}_h\|_0 \|\boldsymbol{w}_h\|_0,$$

where L_1' and L_2' are the constants defined in (62).

Proof Using the skew-symmetry property of the nonlinear terms we have

$$\begin{aligned}(\boldsymbol{g}^n(\boldsymbol{v}_h, \boldsymbol{w}_h), \boldsymbol{w}_h) =& (B(\boldsymbol{v}_h, \tilde{\boldsymbol{u}}_h^n), \boldsymbol{w}_h) \\ \le& \|\nabla \tilde{\boldsymbol{u}}_h^n\|_\infty \|\boldsymbol{v}_h^n\|_0 \|\boldsymbol{w}_h\|_0 + \frac{1}{2}\|\nabla \cdot \boldsymbol{v}_h\|_0 \|\tilde{\boldsymbol{u}}_h^n\|_\infty \|\boldsymbol{w}_h\|_0.\end{aligned} \tag{64}$$

We now observe that applying (4) and (14), one finds for $j = 1, \dots, N$

$$\begin{aligned}\|\tilde{\boldsymbol{u}}_h^j\|_\infty \le& \|\tilde{\boldsymbol{e}}_h^j\|_\infty + \|\boldsymbol{s}_h^j\|_\infty \le C h^{-d/2} \|\tilde{\boldsymbol{e}}_h^j\|_0 + \|\boldsymbol{s}_h^j\|_\infty \le C\left(h^{-d/2}\|\tilde{\boldsymbol{e}}_h^j\|_0 + \|\boldsymbol{u}(t_j)\|_2\right) \\ \le& C\left(h^{-d/2} e^{\hat{L}t_j/2}(C_1 h^k + \Delta t(C_2 + (\Delta t)^2 C_3))^{1/2} + \|\boldsymbol{u}(t_j)\|_2\right),\end{aligned}$$

where in the last inequality we have applied (29). Assuming $h^{-d/2}h^k \le C$ and $h^{-d/2}\Delta t \le C$ we can write

$$\|\tilde{\boldsymbol{u}}_h^j\|_\infty \le C(C_4 + \|\boldsymbol{u}(t_j)\|_2), \tag{65}$$

where C_4 is the constant defined in (61). Arguing similarly, applying again (4) and (14), we also get

$$\|\nabla \tilde{\boldsymbol{u}}_h^j\|_\infty \le \|\nabla \tilde{\boldsymbol{e}}_h^j\|_\infty + \|\nabla \boldsymbol{s}_h^j\|_\infty \le C\left(h^{-d/2-1}\|\tilde{\boldsymbol{e}}_h^j\|_0 + \|\nabla \boldsymbol{u}(t_j)\|_\infty\right).$$

Assuming $h^{-d/2-1+k} \le C$ and $h^{-d/2-1}\Delta t \le C$ we get

$$\|\nabla \tilde{\boldsymbol{u}}_h^j\|_\infty \le C(C_4 + \|\nabla \boldsymbol{u}(t_j)\|_\infty). \tag{66}$$

Now, the statement of the Lemma follows from (64), (65) and (66). □

Remark 3 Observe that condition (63) means that for $d = 2$ we need $\Delta t = O(h^2)$ and $k \ge 2$ to get the error bounds for the pressure and even stronger conditions for $d = 3$ (bounds valid from cubics and with $\Delta t = O(h^{5/2})$). Thus, assuming (63) from (64) it follows that

We are now in position to obtain a first bound of $d_t \tilde{\boldsymbol{e}}_h^n$. It is given by the following result.

Lemma 11 Let $\hat{L}'$ denote $\hat{L}' = 1 + 4(L_1' + (L_2')^2/\mu)$, where L_1' and L_2' are the constants defined in (62). Then, in the conditions of Lemma 10, the following bound holds

$$\begin{aligned}\|d_t\tilde{\boldsymbol{e}}_h^n\|_0^2 + (\Delta t)^2\|\nabla d_t\epsilon_h^n\|_0^2 \le & Ce^{\hat{L}'t_n}\Big(\|d_t\tilde{\boldsymbol{e}}_h^1\|_0^2 + \frac{\mu}{2}\Delta t\|\nabla\cdot d_t\tilde{\boldsymbol{e}}_h^1\|_0^2 + (\Delta t)^2\|\nabla d_t\epsilon_h^1\|_0^2 \\ & + (\Delta t)^2\Big(\big(\hat{C}_1 + \hat{C}_3\big)h^{2k} + \big(\hat{C}_2 + \hat{C}_4)(\Delta t)^2\big)\Big) \\ & + (\Delta t)^2 h^{-2} e^{\hat{L}T}\Big(C_1 h^{2k} + (C_2 + C_3)(\Delta t)^2\big)\Big)C_5\Big),\end{aligned} \tag{67}$$

where

$$C_5 = \int_0^T \|\boldsymbol{u}_t\|_2^2\,dt. \tag{68}$$

Proof We apply Lemma 2 to (49–50) with $\boldsymbol{w}_h^n = d_t\tilde{\boldsymbol{e}}_h^{n+1}$, $y_h^n = d_t\epsilon_h^{n+1}$, $\boldsymbol{g}^n$ defined in (60),

$$\boldsymbol{b}_h^n = d_t\tau_{h,1}^{n+1} + d_t\tau_{h,2}^{n+1} + \tau_{h,6}^{n+1}, \qquad d_h^n = d_t\tau_{h,3}^{n+1} + d_t\tau_{h,4}^{n+1}, \qquad \text{and} \quad r_h^n = d_t\tau_{h,5}^{n+1}.$$

In view of the Lemmas 8, 9 and 10, we only need to bound

$$\tau_{6,h}^{k+1} = B(\tilde{\boldsymbol{e}}_h^k, d_t\boldsymbol{s}_h^{k+1}) + B(d_t\boldsymbol{s}_h^k, \tilde{\boldsymbol{e}}_h^k).$$

For that purpose we write

$$\begin{aligned}\|\tau_{6,h}^{k+1}\|_0 \quad \le \quad & C\|\tilde{\boldsymbol{e}}_h^k\|_{L^{2d}}\|\nabla d_t\boldsymbol{s}_h^{k+1}\|_{L^{2d/(d-1)}} + \frac{1}{2}\|\nabla\cdot\tilde{\boldsymbol{e}}_h^k\|_0\|d_t\boldsymbol{s}_h^{k+1}\|_\infty \\ & + \|\nabla\tilde{\boldsymbol{e}}_h^k\|_0\|d_t\boldsymbol{s}_h^k\|_\infty + \|\tilde{\boldsymbol{e}}_h^k\|_{L^{2d}}\|\nabla\cdot d_t\boldsymbol{s}_h^k\|_{L^{2d/(d-1)}}.\end{aligned}$$

Using inverse inequality (4), the estimate of $\|\tilde{\boldsymbol{e}}_h^k\|_0$ in (29), Hölder's inequality and Sobolev's inequality (2), we get

$$\begin{aligned}\|\tau_{6,h}^{k+1}\|_0^2 \quad & \le \quad C(h^{-(d-1)} + h^{-2})\|\tilde{\boldsymbol{e}}_h^k\|_0^2\Delta t\int_{t_k}^{t_{k+1}}\|\boldsymbol{u}_t\|_2^2\,dt \\ & \le \quad Ch^{-2}e^{\hat{L}t_k}\Big(C_1h^{2k} + (\Delta t)^2(C_2 + (\Delta t)^2C_3)\Big)\Delta t\int_{t_k}^{t_{k+1}}\|\boldsymbol{u}_t\|_2^2\,dt.\end{aligned}$$

Multiplying by Δt and summing from $k = 1$ onwards we have

$$\Delta t\sum_{k=2}^n\|d_t\tau_{6,h}^k\|_0^2 \le Ch^{-2}(\Delta t)^2e^{\hat{L}T}\Big(C_1h^{2k} + (C_2 + C_3)(\Delta t)^2\Big)\int_0^T\|\boldsymbol{u}_t\|_2^2\,dt,$$

and the proof is finished. □

Now, we need to bound the initial errors in the first line in (67). We can assume $\tilde{\boldsymbol{e}}_h^0 = \boldsymbol{e}_h^0 = 0$ since this means we take as initial condition $\boldsymbol{s}_h^0$. Then, $d_t\tilde{\boldsymbol{e}}_h^1 = \tilde{\boldsymbol{e}}_h^1$ and $d_t\boldsymbol{e}_h^1 = \boldsymbol{e}_h^1$. We will also assume $\epsilon_h^{-1} = \epsilon_h^0 = 0$ which means $p_h^0 = \pi_h p^0$.

Lemma 12 *Assume* $\tilde{\boldsymbol{u}}_h^0 = \tilde{\boldsymbol{u}}_h^0 = \boldsymbol{s}_h^0$ *and* $p_h^0 = \pi_h p^0$*, so that* $d_t\tilde{\boldsymbol{e}}_h^1 = \tilde{\boldsymbol{e}}_1$ *and* $d_t\epsilon_h^1 = \epsilon_h^1$*. Then*

$$\begin{aligned}\|d_t\tilde{\boldsymbol{e}}_h^1\|_0^2 + \Delta t\mu\|\nabla\cdot d_t\tilde{\boldsymbol{e}}_h^1\|_0^2 + (\Delta t)^2\|\nabla d_t\epsilon_h^1\|_0^2 & \\ \leq C(\Delta t)^2\Big(\big((1+\mu)(1+h^{-2})C_1 + C_0\|\boldsymbol{u}_t\|_{L^\infty(H^k)}\big)\big)h^{2k} & \\ + \big(\|\boldsymbol{u}_t\|_{L^\infty(H^1)} + \|\boldsymbol{u}_{tt}\|_{L^\infty(L^2)} + C_2 + h^{-2}\Delta t C_3\big)(\Delta t)^2\Big). &\end{aligned} \tag{69}$$

Proof From (21) with $n = 0$ and taking $\boldsymbol{v}_h = \tilde{\boldsymbol{e}}_h^1$ and applying inverse inequality (4) we get

$$\begin{aligned}\|\tilde{\boldsymbol{e}}_h^1\|_0^2 + \Delta t\nu\|\nabla\tilde{\boldsymbol{e}}_h^1\|_0^2 + \Delta t\mu\|\nabla\cdot\tilde{\boldsymbol{e}}_h^1\|_0^2 \leq \Delta t|(B(\tilde{\boldsymbol{u}}_h^0,\tilde{\boldsymbol{u}}_h^1) - B(\boldsymbol{s}_h^0,\boldsymbol{s}_h^1),\tilde{\boldsymbol{e}}_h^1)| & \\ + \Delta t\|\tilde{\boldsymbol{e}}_h^1\|_0(\|\tau_{1,h}^1\|_0 + \|\tau_{2,h}^1\|_0 + C_{\rm inv}h^{-1}(\|\tau_{3,h}^1\|_0 + \|\tau_{4,h}^1\|_0)). &\end{aligned}$$

Now, let us observe that

$$(B(\tilde{\boldsymbol{u}}_h^0,\tilde{\boldsymbol{u}}_h^1) - B(\boldsymbol{s}_h^0,\boldsymbol{s}_h^1),\tilde{\boldsymbol{e}}_h^1) = (B(\tilde{\boldsymbol{e}}_h^0,\boldsymbol{s}_h^1),\tilde{\boldsymbol{e}}_h^1) + (B(\tilde{\boldsymbol{u}}_h^0,\tilde{\boldsymbol{e}}_h^1),\tilde{\boldsymbol{e}}_h^1) = 0,$$

since we have assumed $\boldsymbol{e}_h^0 = 0$ and used the skew-symmetric property of the nonlinear term (16). Then, we can easily get

$$\begin{aligned}\frac{1}{2}\|\tilde{\boldsymbol{e}}_h^1\|_0^2 + \Delta t\nu\|\nabla\tilde{\boldsymbol{e}}_h^1\|_0^2 + \Delta t\mu\|\nabla\cdot\tilde{\boldsymbol{e}}_h^1\|_0^2 \leq & C(\Delta t)^2(\|\tau_{1,h}^1\|_0^2 + \|\tau_{2,h}^1\|_0^2) \\ & + C(\Delta t)^2h^{-2}(\|\tau_{3,h}^1\|_0^2 + \|\tau_{4,h}^1\|_0^2).\end{aligned} \tag{70}$$

For $\tau_{1,h}^1$ and $\tau_{2,h}^n$ from (36) and (42) we deduce

$$\begin{aligned}\|\tau_{1,h}\|_0 &\leq Ch^k\|\boldsymbol{u}_t\|_{L^\infty(H^k)} + \Delta t\|\boldsymbol{u}_{tt}\|_{L^\infty(L^2)}, \\ \|\tau_{2,h}\|_0 &\leq C_1h^k + C_0\Delta t\|\boldsymbol{u}_t\|_{L^\infty(H^1)}\end{aligned}$$

and, thus, using the bounds (37) and (38) for $\tau_{3,h}^n$ and $\tau_{4,h}^n$, from (70) it follows that $\|\tilde{\boldsymbol{e}}_h^1\|_0^2 + \Delta t\nu\|\nabla\tilde{\boldsymbol{e}}_h^1\|_0^2$ is bounded by the right-hand side of (69). To bound $(\Delta t)^2\|\nabla d_t\epsilon_h^1\|_0$ we recall that since we are assuming $\epsilon_h^0 = 0$ we have $d_t\epsilon_h^1 = \epsilon_h^1$, and then we take $q_h = \Delta t\epsilon_h^1$ in (22) for $n = 0$. After integration by parts we get

$$(\Delta t)^2\|\nabla\epsilon_h^1\|_0^2 \leq -\Delta t(\tilde{\boldsymbol{e}}_h^1,\nabla\epsilon_h^1) - (\Delta t)^2(\nabla\tau_{5,h}^1,\nabla\epsilon_h^1),$$

from where it follows that

$$(\Delta t)^2\|\nabla\epsilon_h^1\|_0^2 \leq C\left(\|\tilde{\boldsymbol{e}}_h^1\|_0^2 + (\Delta t)^2\|\nabla\tau_{5,h}^1\|_0^2\right).$$

Now, with the estimate of $\tau_{5,h}$ in (39) the proof is finished. □

Let us gather the constants depending on $\boldsymbol{u}$ and p featuring in the previous bounds in the following two,

$$C_1' = \Big((1 + e^{2\hat{L}T}C_5)C_1 + \hat{C}_1 + \hat{C}_3 + C_0\|\boldsymbol{u}_t\|_{L^\infty(H^k)}\Big)^{1/2}, \tag{71}$$

$$C_2' = \Big((1 + e^{2\hat{L}T}C_5)(C_2 + C_3) + \hat{C}_2 + \hat{C}_4 + \|\boldsymbol{u}_t\|_{L^\infty(H^1)} + \|\boldsymbol{u}_{tt}\|_{L^\infty(L_2)}\Big)^{1/2} \tag{72}$$

where, let us recall, C_0, C_1, C_2, and C_3 are defined in (25–28), $\hat{L}$ in Proposition 1, C_4 in (61), $\hat{C}_1$, $\hat{C}_2$ and $\hat{C}_3$ in (55–58), and C_5 in (68). We notice then that from (90), and Lemmas 11 and 12, and as long as $\tilde{u}_h^0 = u_h^0 = \boldsymbol{s}_h^0$ and $p_h^0 = \pi_h p^0$ and condition (63) holds, it follows that

$$h \left\| \frac{\boldsymbol{e}_h^{n+1} - \boldsymbol{e}_h^n}{\Delta t} \right\|_0 \leq e^{\hat{L}' t_{n+1}} (C_1' h^k + C_2' \Delta t), \tag{73}$$

where $\hat{L}'$ is defined in Lemma 11.

Theorem 2 *Assume that $\tilde{u}_h^0 = u_h^0 = \boldsymbol{s}_h^0$ and $p_h^0 = \pi_h p^0$ and condition (63) holds. Then, the following bound holds*

$$\beta_0^2(\Delta t) \sum_{j=1}^{N} \|p_h^n - \pi_h p^n\|_0^2 \leq C(1+\mu^{-1}) e^{\hat{L}' t_{n+1}} (C_1' h^k + C_2' \Delta t),$$

where $\hat{L}'$ is defined in Lemma 11 and C_1' and C_2' in (71–72).

Proof From the different terms on the right-hand side of (89) we have already estimated the first one in (73). We observe that the truncation errors in (89) can be bounded as $\|\tau_{j,h}^{n+1}\|_{-1} \leq \|\tau_{j,h}^{n+1}\|_0$, $j = 1, 2$ and then apply (36) and (42). We have already estimated $\hat{\tau}_{h,3}$ in (44) and $\tau_{h,4}$ in (38). Then, it only remains to get a bound for the nonlinear term in (89). Arguing as in [26, (48)] we get

$$\begin{aligned}
\|B(\tilde{\boldsymbol{u}}_h^n, \tilde{\boldsymbol{u}}_h^{n+1}) - B(\boldsymbol{s}_h^n, \boldsymbol{s}_h^{n+1})\|_{-1} \leq & \|B(\tilde{\boldsymbol{u}}_h^n, \tilde{\boldsymbol{e}}_h^{n+1})\|_{-1} + \|B(\tilde{\boldsymbol{e}}_h^n, \boldsymbol{s}_h^{n+1})\|_{-1} \\
\leq & C(\|\tilde{\boldsymbol{u}}_h^n\|_\infty + \|\nabla \cdot \tilde{\boldsymbol{u}}_h^n\|_{L^{2d/(d-1)}}) \|\tilde{\boldsymbol{e}}_h^{n+1}\|_0, \\
& + C(\|\boldsymbol{s}_h^{n+1}\|_\infty \|\tilde{\boldsymbol{e}}_h^n\|_0 + \|\boldsymbol{s}_h^{n+1}\|_{L^{2d/(d-1)}} \|\nabla \cdot \tilde{\boldsymbol{e}}_h^n\|_0).
\end{aligned}$$

Now observe that $\|\tilde{\boldsymbol{u}}_h^n\|_\infty$ is bounded in (65), and in view of how $\|\nabla \boldsymbol{s}_h\|_{L^{2d/(d-1)}}$ is bounded in (41), we can estimate $\|\nabla \cdot \tilde{\boldsymbol{u}}_h^n\|_{L^{2d/(d-1)}}$ arguing as in the proof of (66). Recalling (14), the proof is finished. □

4 Numerical Experiments

We present some numerical experiments that corroborate the results in previous section, both with respect to the orders of convergence and the independence of ν of the error constants. As it is customary for these purposes, we will use an example with a known solution. We also present some results on a well-known benchmark problem. In all cases, computations were done in Matlab and the codes were written by ourselves. Linear systems were solved by direct linear algebra as provided by Matlab.

4.1 Problem with known solution

We consider the Navier-Stokes equations in $\Omega = [0,1]^2$ and $T = 5$, with $\boldsymbol{f}$ chosen so that the solution $\boldsymbol{u}$ and p are given by

$$\boldsymbol{u}(x,y,t) = \frac{6+4\cos(4t)}{10} \begin{bmatrix} 8\sin^2(\pi x)(2y(1-y)(1-2y) \\ -8\pi \sin(2*\pi x)(y(1-y))^2 \end{bmatrix} \tag{74}$$

$$p(x,y,t) = \frac{6+4\cos(4t)}{10} \sin(\pi x)\cos(\pi y). \tag{75}$$

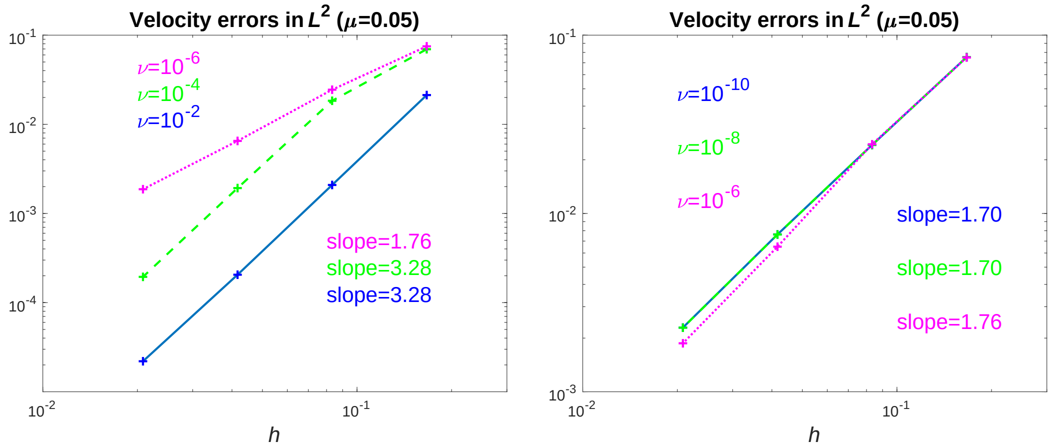

Figure 1: Velocity errors (76) for $T = 5$ and $\mu = 0.05$. Left, large to moderate viscosity. Right moderate to small viscosity.

We used P_2/P_1 pair of mixed finite-elements on a regular triangulation with SW-NE diagonals. We used meshes with $N = 6$, 12, 24 and 48 subdivisions in each coordinate directions. The value of Δt was set to $\Delta t = 0.05$ for the coarser mesh, and divided by 8 every time N was doubled. Repeating the experiments with values of Δt twice as large showed hardly any difference in the errors. Furthermore, for $\nu \leq 10^{-6}$ there was no difference between the results shown here and those obtained by dividing Δt by four every time N was doubled. All this suggests that in the errors shown in the figures below the dominant part comes from the spatial discretization. In the first three figures we show errors

$$\max_{0\leq n\leq N} \|\boldsymbol{u}_h^n - I_h(\boldsymbol{u}^n)\|_0, \qquad \text{for } N = T/\Delta t, \tag{76}$$

where I_h is the standard Lagrange interpolant. The grad-div parameter μ was set to $\mu = 0.05$, since this was the optimal value (marginally, though) among the few we tried from $\mu = 0.01$ to $\mu = 10$. For the nonlinear term, we used $((2\boldsymbol{u}^n - \boldsymbol{u}^{n-1}) \cdot \nabla)\boldsymbol{u}^{n+1}$ instead of $B(\boldsymbol{u}^n, \boldsymbol{u}^{n+1})$, so that the $O(\Delta t)$ expected decay of the errors is due to the discretization of the time derivative $\partial_t \boldsymbol{u}$. We remark that for $\mu = 0.05$ we did not notice any significant difference between the results presented here and those with $B(2\boldsymbol{u}^n - \boldsymbol{u}^{n-1}, \boldsymbol{u}^{n+1})$. For the case $\mu = 0$ in Fig. 2, though we used $B(2\boldsymbol{u}^n - \boldsymbol{u}^{n-1}, \boldsymbol{u}^{n+1})$, since the skew symmetry of B was crucial to keep L^2 errors bounded for small values of ν. In Fig. 1 we present velocity errors (76) for $T = 5$, for different values of the viscosity ν. We also show the slopes of a least-squares fit to the results on the last three meshes. We observe that whereas for $\nu = 10^{-2}$ and 10^{-4} the errors are $O(h^3)$ (although with an apparent $O(\nu^{-1/2})$ dependence), for $\nu = 10^{-6}$ or smaller the results show no significant dependence on ν, and errors almost show the second order convergence predicted in the theory. The contrast with the absence of grad-div stabilization, $\mu = 0$, is sharp, as it can be seen by comparing the results in Fig. 2 with those in Fig. 1. Although there may be some similarities for the case $\nu = 10^{-2}$, these soon disappear as ν is reduced, and errors do not show any significant decay for the values of h considered for $\nu \leq 10^{-4}$.

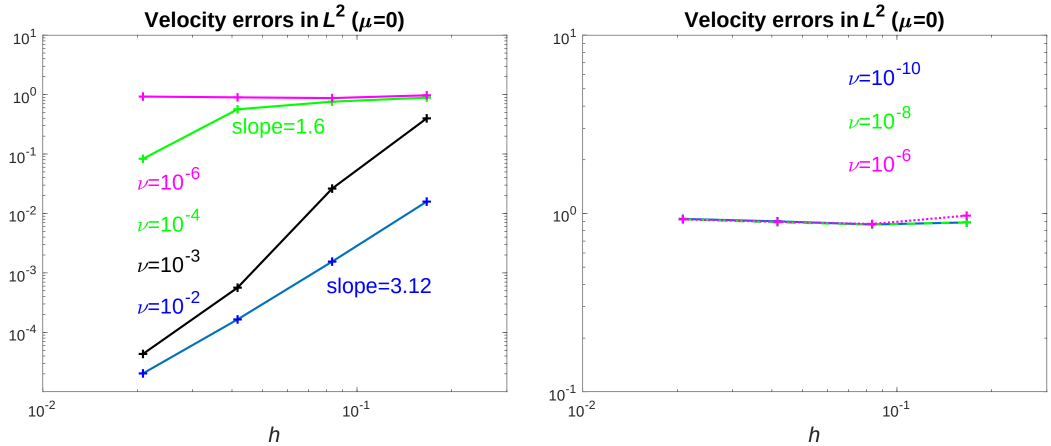

Figure 2: Velocity errors (76) for $T = 5$ and $\mu = 0$. Left, large to moderate viscosity. Right moderate to small viscosity.

In Fig. 3 for $\nu = 10^{-6}$ and $\mu = 0.05$, we show velocity errors (76) and pressure errors

$$\left(\Delta t \sum_{j=1}^{T/\Delta t} \|p_h^n - I_h(p^n)\|_0^2\right)^{1/2} \tag{77}$$

where I_h is the standard Lagrange interpolant, for mixed pairs quadratic velocity and linear pressure and cubic velocity and cuadratic pressure. As our analysis predicts, orders of convergence are one unit higher for the second pair of elements.

Although our analysis suggests that due to factors μ and $1/\mu$ on the right-hand side of the error bounds it is advisable to keep μ independent of h, some researchers find it odd that μ should not depend on h. Results on the left plot in Fig. 4 seem to reinforce that point of view, since taking $\mu = 0.05h$ do not significantly alter the velocity errors of $\mu = 0.05$. However, in view of error constant C_1 in (26) this may be due to the fact that the second spatial derivatives of the pressure are of moderate size. If we alter the right-hand side $\boldsymbol{f}$ in the Navier-Stokes equations so that the velocity is as in (74) but the pressure is

$$p(x, y, t) = 10(6 + 4\cos(4t))\sin(2\pi x)\cos(3\pi y), \tag{78}$$

the term $\mu^{-1}\max_{0\le t\le T}\|p(t)\|_k^2$ makes a significant contribution to the constant C_1, as in can be seen in the right plot on Fig. 4, where the errors when $\mu = 10h$ have a lower rate of decay with h as compared to those of $\mu = 10$ (the value that produced marginally better results from those tried between $\mu = 1$ and $\mu = 100$). Thus, although making μ depend on h may not damage results with respect those of fixed μ in some cases, it may considerably worsen them in some other cases, so that, in accordance with the analysis, it seems to be advisable to take μ independent of h.

Finally, we check if the time step restriction (63) is sharp in practice or if it is a consequence of the limited techniques of analysis. In Fig. 5 we show the errors (77) when Δt is taken proportional to h^2 to h and to $h^{1/2}$. Notice that only $\Delta t = Ch^2$ satisfies restriction (63). The slopes shown correspond to the line joining results of

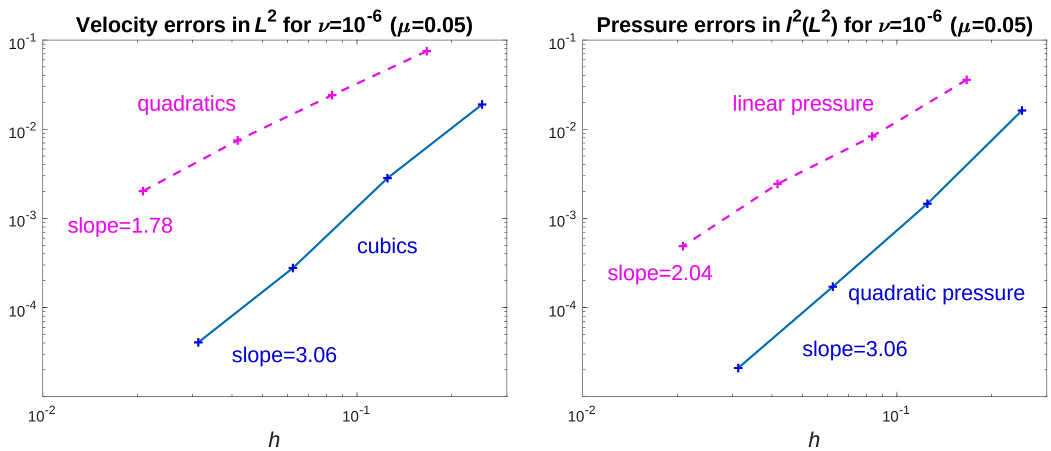

Figure 3: Velocity errors (76) (left) and pressure errors (77) (right) for quadratic and cubic velocity approximation (linear and quadratic pressure approximation, respectively).

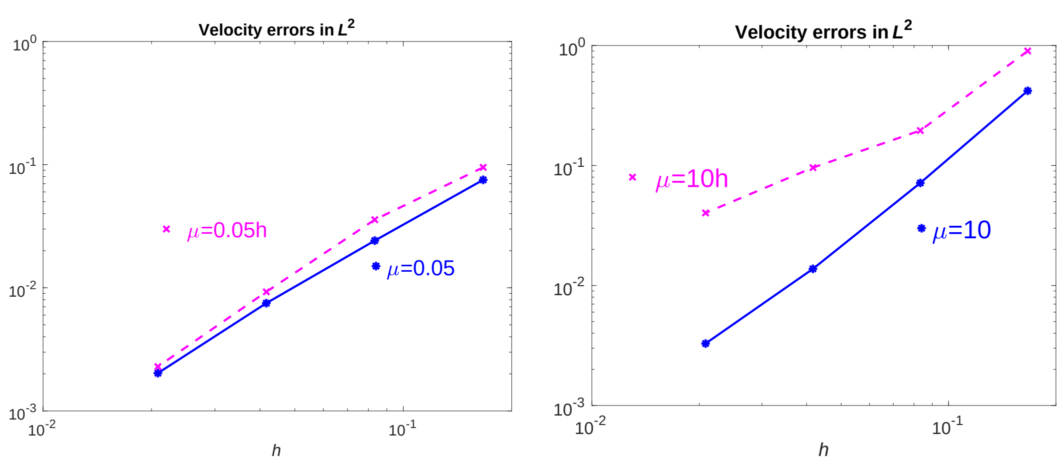

Figure 4: Velocity errors (76) for $\nu = 10^{-6}$. Left, pressure as in (75). Right, pressure as in (78).

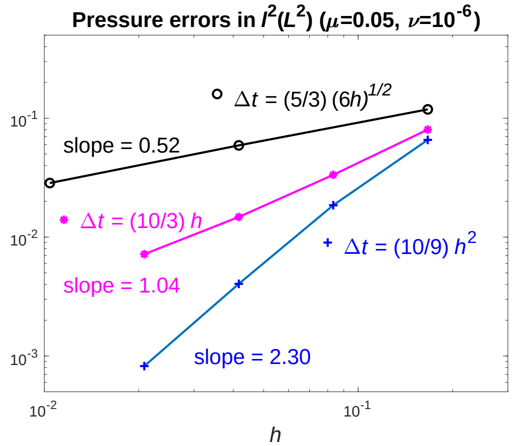

Figure 5: Pressure errors for $\nu = 10^{-6}$.

the two finest meshes. It can be seen that errors decay like Δt in all three cases, suggesting that (63) is not sharp in practice, but rather a limitation imposed by the techniques of analysis.

4.2 Flow past a cylinder

We consider the well-known benchmark problem defined in [46]. The domain is

$$\Omega = (0, 2.2) \times (0, 0.41) / \left\{(x, y) \mid (x - 0.2)^2 + (y - 0.2)^2 \leq 0.0025\right\}$$

and the time interval $[0, 8]$. In both vertical sides the velocity is given by

$$\boldsymbol{u}(0, y) = \boldsymbol{y}(2.2, y) = \frac{6}{0.41^2} \sin\left(\frac{\pi t}{8}\right) \begin{pmatrix} y(0.41 - y) \\ 0 \end{pmatrix},$$

while in the rest of the boundary it is set $\boldsymbol{u} = \mathbf{0}$. Also, at $t = 0$, the initial velocity is $\boldsymbol{u} = \mathbf{0}$. The kinematic viscosity is set to $\nu = 10^{-3}$ and the forcing term is $\boldsymbol{f} = \mathbf{0}$.

It is well-known that around $t = 4$ a vortex sheet develops behind the cylinder, as it can be seen in Fig. 6 when we show the speed and velocity field for $t = 5$ to $t = 8$. The four plots of the velocity fields are plotted in the same scale, and we obtain virtually the same plots as in [35, Fig. 2]

We present errors in maximum values of the drag and lift coefficients c_d and c_l respectively, and the difference of the pressure

$$\Delta p(t) = p(0.15, 0.2, t) - p(0.25, 0.2, t)$$

between the front and the back of the cylinder at $t = 8$

We also computed errors in the times t_d and t_l where the lift and drag coefficients, respectively, attained their maximum values. To compute all these errors, reference values are taken from [35]. Also, following suggestions in [35], we compute c_d and c_l as

$$c_d(t) = -20\big(\nu(\nabla \boldsymbol{u}(t), \nabla \boldsymbol{v}_d) + b(\boldsymbol{u}(t), \boldsymbol{u}(t), \boldsymbol{v}_d) - (p(t), \nabla \cdot \boldsymbol{v}_d)\big),$$
$$c_l(t) = -20\big(\nu(\nabla \boldsymbol{u}(t), \nabla \boldsymbol{v}_l) + b(\boldsymbol{u}(t), \boldsymbol{u}(t), \boldsymbol{v}_l) - (p(t), \nabla \cdot \boldsymbol{v}_l)\big),$$

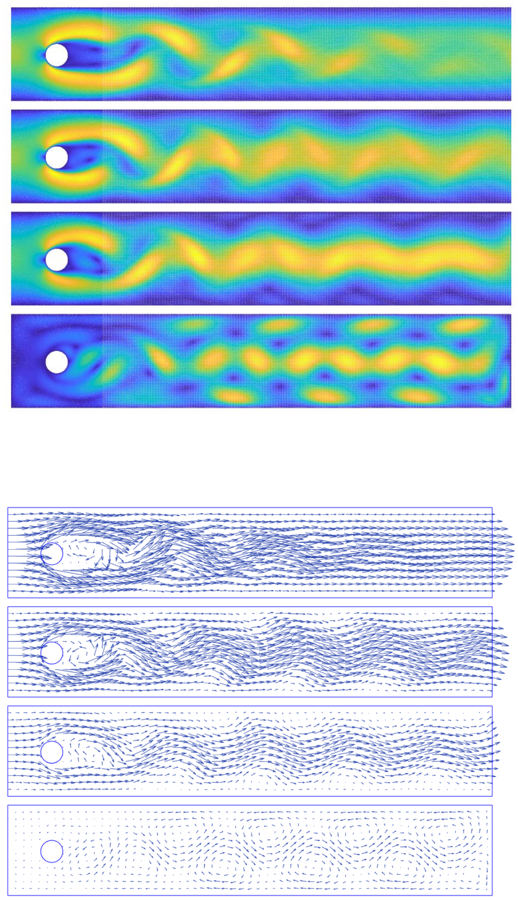

Figure 6: Speed contours (left) and velocity field for times $t = 5, 6, 7, 8$ (from top to bottom).

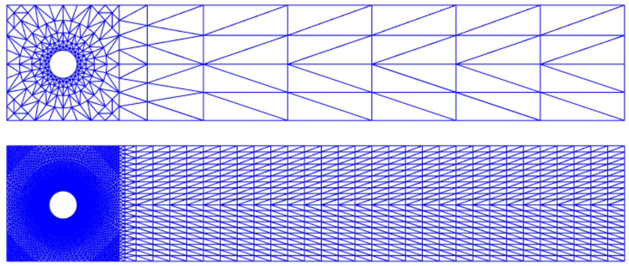

Figure 7: Coarsest and finest meshes used in Fig. 9.

where $\boldsymbol{v}_d$ and $\boldsymbol{v}_l$ are piecewise linear functions vanishing on triangles without vertices on the circumference $c \equiv (x-0.2)^2 + (y-0.2)^2 = 0.0025$. and taking values $\boldsymbol{v}_d = [1,0]^T$ and $\boldsymbol{v}_l = [0,1]^T$ on those nodes on circumference c.

We computed approximations on a sequence of five meshes the coarsest and finest ones being shown in Fig. 7. The total number of degrees of freedom (dgf) of the approximations to the velocity and pressure on these grids are 2057, 4208, 7709, 16961, 46265, so that they are coarser than those used in [35]. We used quadratic isoparametric elements for the velocity and linear elements for pressure. We present results corresponding to $\mu = 0$ and $\mu = 0.01$. This last value was chosen for producing the best results among those with which we tried on one of the grids, the fourth one from coarser to finer, as it can be seen in Table 1 in Appendix B. For each mesh, decreasing values of Δt were tried until the first two digits in the computed error no longer changed. The computed quantities on each grid and for every value of Δt are shown in in Tables 2 and 3 in Appendix B. In the present section, we present some plots corresponding to the smallest values of Δt for each grid in those tables.

In Fig. 8 we show the evolution of the drag and lift coefficients and of $\Delta p(t)$ for $\mu = 0.01$ in blue and for $\mu = 0$ in magenta. This plots should be compared with [35, Fig. 4]. The reference values (taken from [35]) of the maximum values $c_{d,\max}$ of the drag coefficient and $c_{l,\max}$ of the lift coefficient are marked with a red asterisk at time $t_{d,\max}$ and $t_{l,\max}$, respectively, where they are achieved, according to [35]. We also mark with a red asterisks the reference value for $\Delta p(8)$. It can be seen that already for the medium sized grid (dgf=7709) the evolution of c_d here (top left plot in Fig. 8) is very much alike to that in [35, Fig. 4], that the reference value of $c_{d,\max}$ is matched, at least visually, and that the results corresponding to $\mu = 0$ are superimposed to those of $\mu = 0.01$.

For the lift coefficient, however, we see that while the results with $\mu = 0.01$ resemble those in [35, Fig. 4] (specially for the two finest grids, for which the corresponding results are presented in the second row) this is clearly not the case when $\mu = 0$. Only for the finest grid (second row, right plot) have the results with $\mu = 0$ a resemblance to those in [35, Fig. 4]. We conclude then that, for the case of the lift coefficient, adding grad-div stabilization does indeed improve accuracy.

For Δp, although the results with $\mu = 0$ and $\mu = 0.01$ seem to coincide on the mid-sized grid with dgf=7709 (bottom left plot in Fig. 8) at closer inspection (bottom right plot in Fig. 8), the results with $\mu = 0.01$ are much closer to the reference value at $t = 8$. This is also the case for the next finer grid, that with

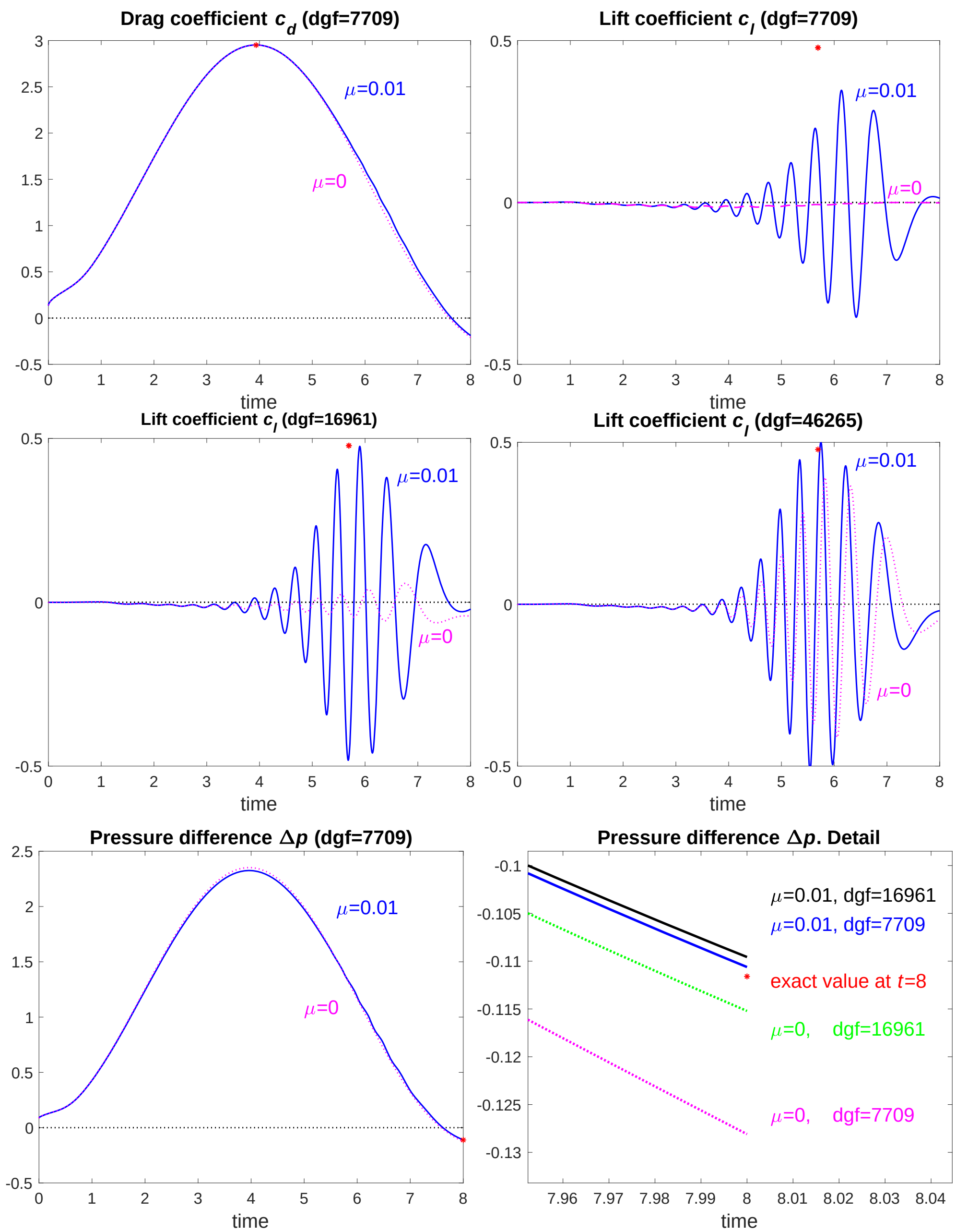

Figure 8: Flow around a cylinder: Evolution of c_d, c_l and Δp.

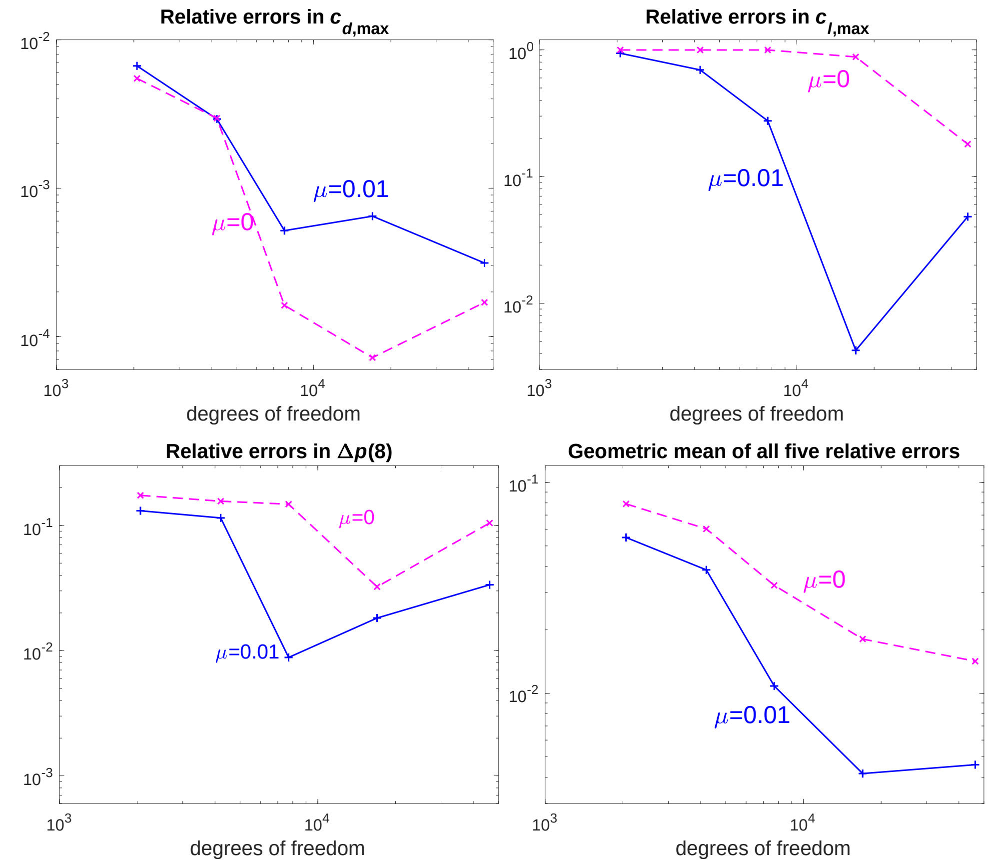

Figure 9: Flow around a cylinder: relative errors. Bottom right plot shows the geometric mean of relative errors in $c_{d,\max}$, $t_{d,\max}$, $c_{l,\max}l$, $t_{l,\max}$ and $\Delta p(8)$.

16961 dgf, for which the corresponding results are also shown.

The plots in the bottom row in Fig. 8 suggest that checking the errors with respect reference values may add further information. In Fig. 9 we present the relative errors in the computation of $c_{d,\max}$, $c_{l,\max}$ and $\Delta p(8)$. It can be seen adding grad-div stabilization worsens the accuracy of the drag coefficient $c_{d,\max}$ (the easiest coefficient to compute accurately, according to [35]), but improves that of the lift coefficient $c_{l,\max}$ (the most difficult one to compute accurately, according to [35]) and $\Delta p(8)$. To have an idea of the overall improvement of adding the grad-div term, we show in the last plot in Fig. 9 the geometric mean of the relative errors in five computed quantities, $c_{d,\max}$, $c_{l,\max}$, $\Delta p(8)$, $t_{d,,\max}$ and $t_{l,\max}$. We can see that, on average, adding the grad-div term improves the overall accuracy in the computation of the five quantities. We notice, however, that as the meshes are refined, the values of the quantities computed with and without the grad-div term seem to get more similar, at least in the case of $c_{d,\max}$ and $c_{l,\max}$. This is in agreement with results in Figs. 1 and 2, where the method with the grad-div term presents better errors only when the viscosity is sufficiently small with respect to the mesh size.

5 Conclusions

In this paper we carry out the error analysis of a fully discrete method for the numerical approximation of the Navier-Stokes equations based on the Euler incremental projection method in time and a Galerkin method plus grad-div stabilization with H^1-conforming inf-sup stable elements in space. Although numerical experimentation in the literature (e.g., [38]) suggests the practical advantages of splitting methods for flows at high Reynolds numbers, the numerical analysis of projection methods where error constants are independent of the Reynolds number is much more scarce. As mentioned in the Introduction, such bounds are obtained only in [11] for the Oseen equations (with $O(h^{k+1/2})$ error decay if equal order elements for velocity and pressure are used) and in [4] for the Navier-Stokes equations, although some needed a priori bounds are yet to be obtained. In the present paper, for the above-mentioned method, we get the optimal rate of convergence in time of order Δt, Δt being the size of the time step. Due to the requirement of error constants independent on the Reynolds number, the error in the pressure is obtained under the assumption $\Delta t \le Ch^{d/2+1}$, $k \ge d/2+1$, d being the spatial dimension and k the degree of the polynomials in the velocity approximation. This restriction, however, seems to be not needed in practice, as it can be observed in the numerical experiments. We want to remark that, concerning the analysis of projection methods, to our knowledge this is the first time a bound for the L^2 norm of the pressure with constants independent on inverse powers of the viscosity is proved for the Navier-Stokes equations. In [11] a bound for a discrete in time primitive of the pressure is proved, which considerably simplifies the pressure error analysis with respect to the standard $L^2(0,T;L^2(\Omega))$ norm (or its discrete counterpart) in which the pressure is usually bounded. In [11] for the explicit treatment of the pressure a condition of type $Ch \le \Delta t$ is required in the error analysis.

We remark that for the spacial discretization we have chosen the simplest (in our opinion) method we know to get bounds with constants independent on inverse powers of the diffusion parameter: a standard method plus grad-div stabilization We prove error bounds of size $O(h^k)$ in space for the L^2 norm of the velocity, the L^2 norm of the divergence of the velocity and a discrete in time L^2 norm of the pressure. Rates of size $O(h^{k+1/2})$ for the L^2 error of the velocity can be found in [12], [27] for methods with continuous interior penalty stabilization and local projection stabilization, respectively, while the question of getting rate $k+1$ is one of the open problems stated in [37]. However, in the present paper, we wanted to concentrate on the analysis of the Euler incremental projection method which is much more complicated to analyze than other standard time integrators, and for this reason we have chosen a simpler stabilization in space and inf-sup stable elements. We want to remark that, on the one hand, the rate $O(h^k)$ we prove for the Galerkin method plus grad-div stabilization is the rate observed in practice in the numerical experiments for small values of the viscosity. On the other hand, we want to remark that for the plain Galerkin method, as it can also be observed in the numerical experiments, error bounds independent on inverse powers of the viscosity cannot be achieved even when approximating very smooth solutions. Finally, results on a well-known benchmark problem, flow around a cylinder, also show that adding the grad-div term noticeably improves the overall accuracy of the numerical approximation.

References

[1] R. A. Adams. *Sobolev spaces.* Academic Press, New York-London, 1975. Pure and Applied Mathematics, Vol. 65.

[2] N. Ahmed, T. Chacón Rebollo, V. John and S. Rubino. Analysis of Full Space-Time Discretization of the Navier–Stokes Equations by a Local Projection Stabilization Method. *IMA J. Numer. Anal.*, 37: 1437–1467, (2017).

[3] D. Arndt, H. Dallmann, and G. Lube. Local projection FEM stabilization for the time-dependent incompressible Navier-Stokes problem. *Numer. Methods Partial Differential Equations*, 31: 1224–1250, 2015.

[4] D. Arndt, H. Dallmann, and G. Lube. Quasi-Optimal Error Estimates for the Incompressible Navier-Stokes Problem Discretized by Finite Element Methods and Pressure-Correction Projection with Velocity Stabilization, arXiv:1609.00807v1.

[5] B. Ayuso, B. García-Archilla and J. Novo. The postprocessed mixed finite-element method for the Navier-Stokes equations. *SIAM J. Numer. Anal.*, 43: 1091–1111, 2005.

[6] S. Badia and R. Codina. Convergence analysis of the FEM approximation of the first order projection method for incompressible flows with and without the inf-sup condition. *Numer. Math.*, 107: 533-557, 2007.

[7] S. C. Brenner and L. R. Scott. *The mathematical theory of finite element methods*, volume 15 of *Texts in Applied Mathematics.* Springer, New York, third edition, 2008.

[8] L. Botti and D. A. Di Pietro. A pressure-correction scheme for convection-dominated incompressible flows with discontinuous velocity and continuous pressure. *J. Comput. Phys.*, 230: 572–585, 2011.

[9] A. L. Bowers, S. Le Borne and L. G. Rebholz. Error analysis and iterative solvers for Navier-Stokes projection methods with standard and sparse grad-dov stabilization. *Comput. Methods Appl. Mech. Engrg.*, 275: 1–19, 2014.

[10] E. Burman. Robust error estimates for stabilized finite element approximations of the two dimensional Navier-Stokes' equations at high Reynolds number. *Comput. Methods Appl. Mech. Engrg.*, 288: 2–23, 2015.

[11] E. Burman, A. Ern and M. A. Fernández. Fractional-Step methods and finite elements with symmetric stabilization for the transient Oseen problem, *ESAIM M2AN*, 51: 487–507, 2017.

[12] E. Burman and M. A. Fernández. Continuous interior penalty finite element method for the time-dependent Navier-Stokes equations: space discretization and convergence. *Numer. Math.*, 107: 39–77, 2007.

[13] E. Burman, M. A. Fernández and P. Hansbo. Continuous interior penalty finite element method for the Oseen's equations. *SIAM J. Numer. Anal.*, 44: 1437–1453, 2006.

[14] T. Chacón Rebollo, M. Gómez Mármol and M. Restelli. Numerical analysis of penalty stabilized finite element discretizations of evolution Navier-Stokes equations. *J. Sci. Comput.*, 63: 885-912, 2015.

[15] S. Charnyi, T. Heister, M. A.Olshanskii and L. G. Rebholz. On conservation laws of Navier-Stokes Galerkin discretizations. *J. Comput. Phys.*, 337: 289–308, 2017.

[16] H. Chen. Pointwise error estimates for finite element solutions of the Stokes problem. *SIAM J. Numer. Anal.*, 44: 1–28, 2006.

[17] P. G. Ciarlet. *The finite element method for elliptic problems.* Studies in Mathematics and its Applications, Vol. 4. North-Holland Publishing Co., Amsterdam, 1978.

[18] R. Codina. Pressure stability in fractional step finite element methods for incompressible flows. *J. Comput. Phys.*, 170: 112–140, 2001.

[19] P. Constantin and C. Foias. *Navier–Stokes Equations*, The University of Chicago Press, Chicago, 1988.

[20] E. D'Agnillo and L. Rebholz. On the enforcement of discrete mass conservation in incompressible flow simulations with continuous velocity approximations. in: Recent advances in scientific computing and applications, Jchun Li, Eric Macharro, Hongtao Yang (eds.), Proceedings of the 8th International COnference on Scientific Computing and Applications, AMS Contemporary Mathematics, vol. 586; 143–152, 2013.

[21] H. Dallmann, D. Arndt and G. Lube. Local projection stabilization for the Oseen problem. *IMA J. Numer. Anal.*, 36: 796–823, 2016.

[22] N. Fehn, W. A. Wall and M. Kronbichler. On the stability of projection methods for the incompressible Navier-Stokes equations based on high-order discontinuous Galerkin discretizations. *J. Comput. Phys.*, 351, 392–421, 2017.

[23] L. P. Franca and T. J. R. Hughes. Two classes of mixed finite element methods. *Comput. Methods Appl. Mech. Engrg.*, 69(1):89–129, 1988.

[24] J. de Frutos V. John and J. Novo. Projection methods for incompressible flow problems with WENO finite difference schemes. *J. Comput. Phys.*, 309: 1–19, 2016.

[25] J. de Frutos, B. García-Archilla, V. John and J. Novo. Grad-div stabilization for the evolutionary Oseen problem with inf-sup stable finite elements. *Journal of Scientific Computing*, 66: 991–1024, 2016.

[26] J. de Frutos, B. García-Archilla, V. John and J. Novo. Analysis of the grad-div stabilization for the time-dependent Navier–Stokes equations with inf-sup stable finite elements. *Advances Comput. Math.*, 44: 195–225, 2018.

[27] J. de Frutos, B. García-Archilla, V. John and J. Novo. Error Analysis of Non Inf-sup Stable Discretizations of the time-dependent Navier–Stokes Equations with Local Projection Stabilization, *IMA J. Numer. Anal.*, (to appear). https://doi.org/10.1093/imanum/dry044.

[28] J. de Frutos, B. García-Archilla and J. Novo. Error analysis of projection methods for non inf-sup stable mixed finite elements. The transient Stokes problem. *Appl. Math. Comput.*, 322: 154–173, 2018.

[29] J. de Frutos, B. García-Archilla and J. Novo. Error analysis of projection methods for non inf-sup stable mixed finite elements. The Navier-Stokes equations. *J. Sci. Comput.*, 74: 426–455, 2018.

[30] V. Girault and P.-A. Raviart. *Finite element methods for Navier-Stokes equations Theory and algorithms.* volume 5 of *Springer Series in Computational Mathematics*. Springer-Verlag, Berlin, 1986.

[31] J. L. Guermond, A. Marra and L. Quartapelle.Subgrid stabilized projection method for 2D unsteady flows at high Reynolds numbers. *Comput. Methods Appl. Mech. Engrg.*, 195: 5857-5876,2006.

[32] J.L. Guermond, P. Minev and J. Shen. An overview of projection methods for incompressible flows. *Comput. Methods Appl. Mech. Engrg.*, 195: 6011-6045, 2006.

[33] J. L. Guermond & L. Quartapelle. On the approximation of the unsteady Navier-Stokes equations by finite element projection methods, *Numer. Math.* 80: 207–238, 1998.

[34] J. G. Heywood and R. Rannacher. Finite element approximation of the nonstationary Navier-Stokes problem. IV. Error analysis for second order time discretization. *SIAM J. Numer. Anal.*, 27: 353–384, 1990.

[35] V. John. Reference values for drag and lift of a two-dimensional time-dependent flow around a cylinder, *Int. J. Numer. Meth. Fluids*, 44: 777–788, 2004.

[36] V. John and A. Kindl. Numerical studies of finite element variational multiscale methods for turbulent flow simulations. *Comput. Methods Appl. Mech. Engrg.*, 199: 841–852, 2010.

[37] V. John, P. Knobloch and J. Novo. Finite elements for scalar convection-dominated equations and incompressible flow problems: a never ending story? *J. Comput. Visual Sci.* (2018). https://doi.org/10.1007/s00791-018-0290-5.

[38] G. Karniadakis and S. Sherwin, *Spectral/hp Element Methods for Computational Fluid Dynamics*, Scd. Edition, Oxford University Press, 2005.

[39] W. Layton, C. Manica, M. Neda & L. Rebholz. On the accuracy of the rotation form in simulations of the Navier-Stokes equations. J. Comput. Phys., 228: 3433-3447, 2009.

[40] A. Linke and L. Rebholz, On a reduced sparsity stabilization of grad-div type for incompressible flow problems *Comput. Methods Appl. Mech. Engrg.*, 261–262: 142–153, 2013.

[41] P. D. Minev. A stabilized incremental projection scheme for the Incompressible Navier-Stokes equations. *Int. J. Numer. Methods Fluids*, 36: 441–464, 2001.

[42] A. Prohl. Projection and Quasi-Compressibility Methods for Solving the Incompressible Navier-Stokes equations, B. G. Teubner, Springer, Stuttgart, 1997.

[43] A. Prohl. On pressure approximations via projection methods for nonstationary incompressible Navier-Stokes equations, *SIAM J. Numer. Anal.*, 29: 158–180, 2008.

[44] R. Rannacher. On Chorin's Projection Method for the Incompressible Navier-Stokes Equations. *Lecture Notes in Mathematics*, vol. 1530. Springer, Berlin (1992).

[45] L. Röhe and G. Lube. Analysis of a variational multiscale method for large-eddy simulation and its application to homogeneous isotropic turbulence. *Comput. Methods Appl. Mech. Engrg.*, 199: 2331–2342, 2010.

[46] M. Schäfer and S. Turek. Benchmark computations of laminar flow around a cylinder, With support by F. Durst, E. Krause, R. Rannacher, in: Flow Simulation with High-Performance Computers II. DFG Priority Research Programme Results 1993–1995, Vieweg, Wiesbaden, 1996, pp.547–566.

[47] P. W.Schroeder and G. Lube. Pressure-robust analysis of divergence-free and conforming FEM for evolutionary incompressible Navier–Stokes flows *J. Num. Anal.*, 25: 249–276, 2017.

[48] J. Shen. On error estimates of projection methods for Navier-Stokes equations: first-order schemes, *SIAM J. Numer. Anal.*, 29: 57–77, 1992.

[49] J. Shen. Remarks on the pressure error estimates for the projection methods. *Numer Math.*, 67: 513–520, 1994.

A Proof of Lemmas 2, 6 and 9

A.1 Proof of Lemma 2

Proof Taking $\boldsymbol{\chi}_h = \Delta t \boldsymbol{w}_h^{n+1}$ in (31) and $\phi_h = \Delta t(2y_h^n - y_h^{n-1})$ in (32) and summing both equations we have

$$\begin{aligned}\frac{1}{2}\left(\|\boldsymbol{w}_h^{n+1}\|_0^2 - \|\boldsymbol{w}_h^n\|_0^2 + \|\boldsymbol{w}_h^{n+1} - \boldsymbol{w}_h^n\|_0^2\right) + \Delta t\big(\nu\|\nabla \boldsymbol{w}_h^{n+1}\|_0^2 + \mu\|\nabla\cdot \boldsymbol{w}_h^{n+1}\|_0^2\big) \\ + (\Delta t)^2(\nabla(y_h^{n+1} - y_h^n), \nabla(2y_h^n - y_h^{n-1})) \\ \le \Delta t\big((\boldsymbol{b}_h^{n+1}, \boldsymbol{w}_h^{n+1}) + (d^{n+1}, \nabla\cdot \boldsymbol{w}_h^{n+1})\big) + (\Delta t)^2(\nabla(2y_h^n - y_h^{n-1})), \nabla r^{n+1}). \quad (79)\end{aligned}$$

By writing $2y_h^n - y_h^{n-1} = y_h^{n+1} - \big((y_h^{n+1} - y_h^n) - (y_h^n - y_h^{n-1})\big)$, for the last term on the left-hand side of (79)) we have

$$\begin{aligned}\big(\nabla(y_h^{n+1} - y_h^n), \nabla(2y_h^n - y_h^{n-1})\big) =& (\nabla(y_h^{n+1} - y_h^n), \nabla y_h^{n+1}) \\ &- \big(\nabla(y_h^{n+1} - y_h^n), \nabla(y_h^{n+1} - y_h^n) - \nabla(y_h^n - y_h^{n-1})\big) \quad (80)\end{aligned}$$

We express the first term on the right-hand side of (80) as follows,

$$(\nabla(y_h^{n+1} - y_h^n), \nabla y_h^{n+1}) = \frac{1}{2}\big(\|\nabla y_h^{n+1}\|_0^2 - \|\nabla y_h^n\|_0^2 + \|\nabla(y_h^{n+1} - y_h^n)\|_0^2\big), \quad (81)$$

and for the second one, using (32) and integration by parts we have

$$\begin{aligned}-\big(\nabla(y_h^{n+1} - y_h^n), \nabla(y_h^{n+1} - y_h^n) - \nabla(y_h^n - y_h^{n-1})\big) \\ = -\frac{1}{\Delta t}\big(\boldsymbol{w}_h^{n+1} - \boldsymbol{w}_h^n, \nabla(y_h^{n+1} - y_h^n)\big) - \big(\nabla(r^{n+1} - r^n), \nabla(y_h^{n+1} - y_h^n)\big) \\ \ge -\frac{1}{2(\Delta t)^2}\|\boldsymbol{w}_h^{n+1} - \boldsymbol{w}_h^n\|_0^2 - \frac{1}{2}\|\nabla(y_h^{n+1} - y_h^n)\|_0^2 \\ -\frac{1}{2\epsilon_1\Delta t}\|\nabla(r^{n+1} - r^n)\|_0^2 - \frac{\epsilon_1\Delta t}{2}\|\nabla(y_h^{n+1} - y_h^n)\|_0^2, \quad (82)\end{aligned}$$

for some $\epsilon_1 > 0$. Observe that the last two terms on the righ-hand side above can be bounded below by

$$-\frac{1}{\epsilon_1\Delta t}\left(\|\nabla r^{n+1}\|_0^2 + \|\nabla r^n\|_0^2\right) - \epsilon_1\Delta t\left(\|y_h^{n+1}\|_0^2 + \|\nabla y_h^n\|_0^2\right).$$

Thus, from (80), (81) and (82) we may bound the last term on the left-hand side of (79) as

$$
\begin{aligned}
(\Delta t)^2\big(\nabla(y_h^{n+1}-y_h^n),\nabla(2y_h^n-y_h^{n-1})\big) \geq{}& \frac{(\Delta t)^2}{2}\big(\|\nabla y_h^{n+1}\|_0^2-\|\nabla y_h^{n+1}\|_0^2\big)\\
&-\frac{1}{2}\|\boldsymbol{w}_h^{n+1}-\boldsymbol{w}_h^n\|_0^2-\frac{\Delta t}{\epsilon_1}\left(\|\nabla r^{n+1}\|_0^2+\|\nabla r^n\|_0^2\right)\\
&-\epsilon_1(\Delta t)^3\left(\|y_h^{n+1}\|_0^2+\|\nabla y_h^n\|_0^2\right).
\end{aligned}
$$

Arguing similary with the last term on the right-hand side of (79) we have

$$
\begin{aligned}
(\Delta t)^2(\nabla(2y_h^n-y_h^{n-1})),\nabla r^{n+1}) \leq{}& (\Delta t)^2\left|(\nabla y_h^{n+1},\nabla r^{n+1})\right|+\Delta t\left|(\boldsymbol{w}_h^{n+1}-\boldsymbol{w}_h^n,\nabla r^{n+1})\right|\\
&-(\Delta t)^2(\nabla(r^{n+1}-r^n),\nabla r^{n+1})\\
={}& (\Delta t)^2\left|(\nabla y_h^{n+1},\nabla r^{n+1})\right|+\Delta t\left|(\boldsymbol{w}_h^{n+1}-\boldsymbol{w}_h^n,\nabla r^{n+1})\right|\\
&\frac{(\Delta t)^2}{2}\left(\|\nabla r^n\|_0^2-\|\nabla(r^{n+1}-r^n)\|_0^2-\|\nabla r^{n+1}\|_0^2\right)\\
\leq{}& \epsilon_2\frac{(\Delta t)^3}{2}\|\nabla(y_h^{n+1})\|_0^2+\epsilon_3\Delta t\big(\|\boldsymbol{w}_h^{n+1}\|_0^2+\|\boldsymbol{w}_h^n\|_0^2\big)\\
&+\Delta t\Big(\frac{1}{2\epsilon_2}+\frac{1}{2\epsilon_3}\Big)\|\nabla r^{n+1}\|_0^2+\frac{(\Delta t)^2}{2}\|\nabla r^n\|_0^2
\end{aligned}
$$

for some $\epsilon_2,\epsilon_3>0$. Then, it follows that (79) can be arranged to

$$
\begin{aligned}
&\frac{1}{2}\big(\|\boldsymbol{w}_h^{n+1}\|_0^2-\|\boldsymbol{w}_h^n\|_0^2\big)+\Delta t\big(\nu\|\nabla\boldsymbol{w}_h^{n+1}\|_0^2+\mu\|\nabla\cdot\boldsymbol{w}_h^{n+1}\|_0^2\big)\\
&\qquad+\frac{(\Delta t)^2}{2}\big(\|\nabla y_h^{n+1}\|_0^2-\|\nabla y_h^n\|_0^2\big)\leq\\
&\Delta t\big((\boldsymbol{b}_h^{n+1},\boldsymbol{w}_h^{n+1})+(d^{n+1},\nabla\cdot\boldsymbol{w}_h^{n+1})\big)\\
&+\Delta t\left(\Big(\frac{1}{\epsilon_1}+\frac{1}{2\epsilon_2}+\frac{1}{2\epsilon_3}\Big)\|\nabla r^{n+1}\|_0^2+\Big(\frac{1}{\epsilon_1}+\frac{\Delta t}{2}\Big)\|\nabla r^n\|_0^2\right)\\
&+(\Delta t)^3\frac{1}{2}\big((2\epsilon_1+\epsilon_2)\|\nabla y_h^{n+1}\|_0^2+2\epsilon_1\|\nabla y_h^n\|_0^2\big)+\epsilon_3\Delta t\big(\|\boldsymbol{w}_h^{n+1}\|_0^2+\|\boldsymbol{w}_h^n\|_0^2\big).
\end{aligned}
\tag{83}
$$

We now choose $\epsilon_1=1/16$ and $\epsilon_2=1/4$ and $\epsilon_3=1/16$, so that $2\epsilon_1+\epsilon_2=3/8$ and $\epsilon_1^{-1}+(\epsilon_2^{-1}+\epsilon_3^{-1})/2=26$. We also have

$$
\Delta t(\boldsymbol{b}_h^{n+1},\boldsymbol{w}_h^{n+1})\leq 2\Delta t\|\boldsymbol{b}_h^{n+1}\|_0^2+\frac{\Delta t}{8}\|\boldsymbol{w}_h^{n+1}\|_0^2,
$$

and

$$
\Delta t(d^{n+1},\nabla\cdot\boldsymbol{w}_h^{n+1})\leq\frac{\Delta t}{2\mu\epsilon_4}\|d^{n+1}\|_0^2+\epsilon_4\Delta t\frac{\mu}{2}\|\nabla\cdot\boldsymbol{w}_h^{n+1}\|_0^2,
$$

for some $\epsilon_4>0$. Then, from (83) it follows that

$$
\begin{aligned}
&\frac{1}{2}\big(\|\boldsymbol{w}_h^{n+1}\|_0^2-\|\boldsymbol{w}_h^n\|_0^2\big)+\Delta t\Big(\nu\|\nabla\boldsymbol{w}_h^{n+1}\|_0^2+\Big(1-\frac{\epsilon_4}{2}\Big)\mu\|\nabla\cdot\boldsymbol{w}_h^{n+1}\|_0^2\Big)\\
&\quad+\frac{(\Delta t)^2}{2}\big(\|\nabla y_h^{n+1}\|_0^2-\|\nabla y_h^n\|_0^2\big)\\
&\qquad\leq\Delta t\left(26\|\nabla r^{n+1}\|_0^2+\Big(16+\frac{\Delta t}{2}\Big)\|\nabla r^n\|_0^2+2\|\boldsymbol{b}_h^{n+1}\|_0^2+\frac{1}{2\mu\epsilon_4}\|d^{n+1}\|_0^2\right)\\
&\qquad\quad+\frac{\Delta t}{16}\left(3\|\boldsymbol{w}_h^{n+1}\|_0^2+\|\boldsymbol{w}_h^n\|_0^2\right)+\frac{(\Delta t)^2}{16}\big(3\|\nabla y_h^{n+1}\|_0^2+\|\nabla y_h^n\|_0^2\big).
\end{aligned}
\tag{84}
$$

Taking $\epsilon_4 = 1$, multiplying by 2 and summing from $n = 0$ onwards and noticing that

$$\frac{\Delta t}{8}\sum_{j=0}^{n}\left(3\|\boldsymbol{w}_h^{n+1}\|_0^2 + \|\boldsymbol{w}_h^{n}\|_0^2\right) = \frac{\Delta t}{8}\|\boldsymbol{w}_h^{0}\|_0^2 + \frac{\Delta t}{2}\sum_{j=1}^{n}\|\boldsymbol{w}_h^{j}\|_0^2 + \frac{3}{8}\Delta t\|\boldsymbol{w}_h^{n+1}\|_0^2$$
$$\leq \frac{\Delta t}{2}\sum_{j=0}^{n+1}\|\boldsymbol{w}_h^{j}\|_0^2,$$

and a similar bound for sum of $(\Delta t)^2\|\nabla y_h^j\|_0^2$, we get

$$\|\boldsymbol{w}_h^{n+1}\|_0^2 + \Delta t\sum_{j=1}^{n+1}\Big(2\nu\|\nabla \boldsymbol{w}_h^{j}\|_0^2 + \mu\|\nabla\cdot\boldsymbol{w}_h^{n+1}\|_0^2\Big) + (\Delta t)^2\|\nabla y_h^{n+1}\|_0^2$$
$$\leq \|\boldsymbol{w}_h^{0}\|_0^2 + (\Delta t)^2\|\nabla y_h^{0}\|_0^2 + \frac{\Delta t}{2}\sum_{j=0}^{n+1}\left(\|\boldsymbol{w}_h^{j}\|_0^2 + (\Delta t)^2\|\nabla y_h^{j}\|_0^2\right)$$
$$+ \Delta t\sum_{j=1}^{n+1}\left(52\|\nabla r^j\|_0^2 + \Big(32+\Delta t\Big)\|\nabla r^{j-1}\|_0^2 + 4\|\boldsymbol{b}_h^j\|_0^2 + \frac{1}{\mu}\|d^j\|_0^2\right).$$

Recall that we are assuming $\Delta t \leq 1$ so that we can bound $32 + \Delta t \leq 33$. Then, applying Lemma 1, the bound (33) easily follows. To prove (35) we write

$$\left|(\boldsymbol{g}^n(\boldsymbol{w}_h^n, \boldsymbol{w}_h^{n+1}), \boldsymbol{w}_h^{n+1})\right| \leq L_1\|\boldsymbol{w}_h^n\|_0\|\boldsymbol{w}_h^{n+1}\|_0 + L_2\|\nabla\cdot\boldsymbol{w}_h^n\|_0\|\boldsymbol{w}_h^{n+1}\|_0$$
$$\leq \frac{L_1}{2}\left(\|\boldsymbol{w}_h^n\|_0^2 + \|\boldsymbol{w}_h^{n+1}\|_0^2\right) + \frac{\mu}{4}\|\nabla\cdot\boldsymbol{w}_h^n\|_0^2 + \frac{L_2^2}{\mu}\|\boldsymbol{w}_h^{n+1}\|_0^2.$$

Then, observe that (84) holds if we add $-\frac{\mu}{4}\|\nabla\cdot\boldsymbol{w}_h^n\|_0^2$ to the left hand side and if, on the right hand side, we replace $\frac{\Delta t}{16}\left(3\|\boldsymbol{w}_h^{n+1}\|_0^2 + \|\boldsymbol{w}_h^{n}\|_0^2\right)$ by

$$\Delta t\left(\Big(\frac{3}{16} + \frac{L_1}{2} + \frac{L_2^2}{\mu}\Big)\|\boldsymbol{w}_h^{n+1}\|_0^2 + \Big(\frac{1}{16} + \frac{L_1}{2}\Big)\|\boldsymbol{w}_h^{n}\|_0^2\right).$$

Thus, taking $\epsilon_4 = 1/2$, multiplying by 2, summing from $n = 0$ onwards and noticing that

$$\Delta t\sum_{j=1}^{n+1}\mu\Big(\frac{3}{2}\|\nabla\cdot\boldsymbol{w}_h^{j}\|_0^2 - \frac{1}{2}\|\nabla\cdot\boldsymbol{w}_h^{j-1}\|_0^2\Big) = -\frac{\mu}{2}\Delta t\|\nabla\cdot\boldsymbol{w}_h^{0}\|_0^2 + \Delta t\sum_{j=1}^{n}\|\nabla\cdot\boldsymbol{w}_h^{j}\|_0^2$$
$$+ \frac{3}{2}\Delta t\|\nabla\cdot\boldsymbol{w}_h^{n+1}\|_0^2$$
$$\geq -\frac{\mu}{2}\Delta t\|\nabla\cdot\boldsymbol{w}_h^{0}\|_0^2 + \Delta t\sum_{j=1}^{n+1}\|\nabla\cdot\boldsymbol{w}_h^{j}\|_0^2,$$

it follows that arguing as before and applying Lemma 1 (35) is proved. □

A.2 Proof of Lemma 6

Proof Using the inf-sup condition (3) and (43) we get

$$\beta_0\|\epsilon_h^{n+1}\|_0 \le \left\|\frac{\boldsymbol{e}_h^{n+1}-\boldsymbol{e}_h^n}{\Delta t}\right\|_{-1} + \nu\|\nabla\tilde{\boldsymbol{e}}_h^{n+1}\|_0 + \|B(\tilde{\boldsymbol{u}}_h^n,\tilde{\boldsymbol{u}}_h^{n+1}) - B(\boldsymbol{s}_h^n,\boldsymbol{s}_h^{n+1})\|_{-1}$$
$$+ \mu\|\nabla\cdot\tilde{\boldsymbol{e}}_h^{n+1}\|_0 + \|\tau_{1,h}^{n+1}\|_{-1} + \|\tau_{2,h}^{n+1}\|_{-1} + \|\hat{\tau}_{3,h}^{n+1}\|_0 + \|\tau_{4,h}^{n+1}\|_0. \quad (85)$$

Let us bound the first term on the right-hand side of (85). Applying (45) we get

$$\left\|\frac{\boldsymbol{e}_h^{n+1}-\boldsymbol{e}_h^n}{\Delta t}\right\|_{-1} \le C\left\|(A_h^{\rm div})^{-1/2}\Pi_h^{\rm div}\Big(\frac{\boldsymbol{e}_h^{n+1}-\boldsymbol{e}_h^n}{\Delta t}\Big)\right\|_0 + Ch\left\|\frac{\boldsymbol{e}_h^{n+1}-\boldsymbol{e}_h^n}{\Delta t}\right\|_0. \quad (86)$$

From (43) and taking into account that $\|A_h^{-1/2}\Pi_h^{\rm div}\mathbf{g}\|_0 \le \|\mathbf{g}\|_{-1}$, for all $\mathbf{g}\in L^2(\Omega)^d$, see [5, (2.16)], for the first term on the right hand side of (86). we get

$$\left\|(A_h^{\rm div})^{-1/2}\Pi_h^{\rm div}\Big(\frac{\boldsymbol{e}_h^{n+1}-\boldsymbol{e}_h^n}{\Delta t}\Big)\right\|_0 \le \nu\|(A_h^{\rm div})^{-1/2}A_h\tilde{\boldsymbol{e}}_h^{n+1}\|_0 + \mu\|(A_h^{\rm div})^{-1/2}C_h\tilde{\boldsymbol{e}}_h^{n+1}\|_0$$
$$+ \|B(\tilde{\boldsymbol{u}}_h,\tilde{\boldsymbol{u}}_h^{n+1}) - B(\boldsymbol{s}_h^n,\boldsymbol{s}_h^{n+1})\|_{-1} \quad (87)$$
$$+ \|\tau_{1,h}^{n+1}\|_{-1} + \|(A_h^{\rm div})^{-1/2}D_h\hat{\tau}_{3,h}^{n+1}\|_0$$
$$+ \|\tau_{2,h}^{n+1}\|_{-1} + \|(A_h^{\rm div})^{-1/2}D_h\tau_{4,h}^{n+1}\|_0.$$

For the first term on the right-hand side of (87) arguing as in [25] we get

$$\begin{aligned}
\|(A_h^{\rm div})^{-1/2}A_h\tilde{\boldsymbol{e}}_h^{n+1}\|_0 &= \sup_{\boldsymbol{v}_h\in V_h^{\rm div},\boldsymbol{v}_h\neq 0}\frac{|(A_h\tilde{\boldsymbol{e}}_h^{n+1},(A_h^{\rm div})^{-1/2}\boldsymbol{v}_h)|}{\|\boldsymbol{v}_h\|_0}\\
&= \sup_{\boldsymbol{v}_h\in V_h^{\rm div},\boldsymbol{v}_h\neq 0}\frac{|(\nabla\tilde{\boldsymbol{e}}_h^{n+1},\nabla(A_h^{\rm div})^{-1/2}\boldsymbol{v}_h)|}{\|\boldsymbol{v}_h\|_0}\\
&\le \sup_{\boldsymbol{v}_h\in V_h^{\rm div},\boldsymbol{v}_h\neq 0}\frac{\|\nabla\tilde{\boldsymbol{e}}_h^{n+1}\|_0\|\nabla(A_h^{\rm div})^{-1/2}\boldsymbol{v}_h\|_0}{\|\boldsymbol{v}_h\|_0}\\
&= \sup_{\boldsymbol{v}_h\in V_h^{\rm div},\boldsymbol{v}_h\neq 0}\frac{\|\nabla\tilde{\boldsymbol{e}}_h^{n+1}\|_0\|\boldsymbol{v}_h\|_0}{\|\boldsymbol{v}_h\|_0} = \|\nabla\tilde{\boldsymbol{e}}_h^{n+1}\|_0.
\end{aligned}$$

Arguing similarly with the other terms in (87) we get

$$\begin{aligned}
\left\|(A_h^{\rm div})^{-1/2}\Pi_h^{\rm div}\Big(\frac{\boldsymbol{e}_h^{n+1}-\boldsymbol{e}_h^n}{\Delta t}\Big)\right\|_0 \le\ & \nu\|\nabla\tilde{\boldsymbol{e}}_h^{n+1}\|_0 + \mu\|\nabla\cdot\tilde{\boldsymbol{e}}_h^{n+1}\|_0\\
&+\|B(\tilde{\boldsymbol{u}}_h,\tilde{\boldsymbol{u}}_h^{n+1}) - B(\boldsymbol{s}_h^n,\boldsymbol{s}_h^{n+1})\|_{-1} \quad (88)\\
&+\|\tau_{1,h}^{n+1}\|_{-1} + \|\hat{\tau}_{3,h}^{n+1}\|_0\\
&+\|\tau_{2,h}^{n+1}\|_{-1} + \|\tau_{4,h}^{n+1}\|_0.
\end{aligned}$$

From (86) and (88) and going back to (85) we get

$$\begin{aligned}
\beta_0\|\epsilon_h^{n+1}\|_0 \le\ & Ch\left\|\frac{\boldsymbol{e}_h^{n+1}-\boldsymbol{e}_h^n}{\Delta t}\right\|_0 + C\nu\|\nabla\tilde{\boldsymbol{e}}_h^{n+1}\|_0 + C\mu\|\nabla\cdot\tilde{\boldsymbol{e}}_h^{n+1}\|_0\\
&+C\|B(\tilde{\boldsymbol{u}}_h^n,\tilde{\boldsymbol{u}}_h^{n+1}) - B(\boldsymbol{s}_h^n,\boldsymbol{s}_h^{n+1})\|_{-1} \quad (89)\\
&+C\|\tau_{1,h}^{n+1}\|_{-1} + C\|\tau_{2,h}^{n+1}\|_{-1} + C\|\hat{\tau}_{3,h}^{n+1}\|_0 + C\|\tau_{4,h}^{n+1}\|_0.
\end{aligned}$$

Finally by subtracting the expression corresponding to $n+1$ and n in (30) we get

$$\boldsymbol{e}_h^{n+1} - \boldsymbol{e}_h^n = (\tilde{\boldsymbol{e}}_h^{n+1} - \tilde{\boldsymbol{e}}_h^n) - \Delta t \nabla (p_h^{n+1} - 2p_h^n + p_h^{n-1}),$$

so that arguing as in Remark 2 we have

$$\left\| \frac{\boldsymbol{e}_h^{n+1} - \boldsymbol{e}_h^n}{\Delta t} \right\|_0 \le \left\| \frac{\tilde{\boldsymbol{e}}_h^{n+1} - \tilde{\boldsymbol{e}}_h^n}{\Delta t} \right\|_0, \tag{90}$$

and (48) follows from (89). □

A.3 Proof of Lemma 9

Proof To bound $d_t \tau_{2,h}^k$ we observe that

$$\begin{aligned} d_t \tau_{2,h}^k \quad = \quad & B(\boldsymbol{u}^k - \boldsymbol{u}^{k-1}, \boldsymbol{u}^k - \boldsymbol{u}^{k-1}) + B(\boldsymbol{u}^k - 2\boldsymbol{u}^{k-1} + \boldsymbol{u}^{k-2}, \boldsymbol{u}^{k-1}) \\ & + B(d_t(\boldsymbol{u}^{k-1} - \boldsymbol{s}_h^{k-1}), \boldsymbol{s}_h^{k-1}) + B(\boldsymbol{u}^{k-1} - \boldsymbol{s}_h^{k-1}, \boldsymbol{s}_h^k - \boldsymbol{s}_h^{k-1}) \\ & + B(\boldsymbol{u}^{k-1} - \boldsymbol{u}^{k-2}, \boldsymbol{u}^{k-1} - \boldsymbol{s}^{k-1}) + B(\boldsymbol{u}^{k-1}, d_t(\boldsymbol{u}^k - \boldsymbol{s}_h^k)). \end{aligned} \tag{91}$$

In what follows, we will use the following bound

$$\|B(\boldsymbol{v}, \boldsymbol{w})\|_0 \le C \|\boldsymbol{v}\|_1 \|\nabla \boldsymbol{w}\|_{L^{2d/(d-1)}} + C \|\nabla \cdot \boldsymbol{v}\|_0 \|\boldsymbol{w}\|_\infty$$

and using Sobolev's bound (2),

$$\|B(\boldsymbol{v}, \boldsymbol{w})\|_0 \le C \|\boldsymbol{v}\|_1 \|\boldsymbol{w}\|_2 + C \|\nabla \cdot \boldsymbol{v}\|_0 \|\boldsymbol{w}\|_2.$$

Notice also that only in the third and forth terms on the right-hand side of (91) the divergence term will be nonzero. For the first two terms on the right-hand side of (91) we have

$$\|B(\boldsymbol{u}^k - \boldsymbol{u}^{k-1}, \boldsymbol{u}^k - \boldsymbol{u}^{k-1})\|_0^2 \le C(\Delta t)^3 \|\boldsymbol{u}_t\|_{L^\infty(H^1)}^2 \int_{t_{k-1}}^{t_k} \|\boldsymbol{u}_t\|_2^2 \, dt,$$

and

$$\|B(\boldsymbol{u}^k - 2\boldsymbol{u}^{k-1} + \boldsymbol{u}^{k-2}, \boldsymbol{u}^{k-1})\|_0^2 \le C(\Delta t)^3 \|\boldsymbol{u}\|_{L^\infty(W^{1,\infty})}^2 \int_{t_{k-2}}^{t_k} \|\boldsymbol{u}_{tt}\|_2^2 \, dt.$$

For the third and fourth term on the right-hand side of (91)), recalling the bounds (14) and (41), and using Sobolev's bound (2) we may write

$$\|B(d_t(\boldsymbol{u}^{k-1} - \boldsymbol{s}_h^{k-1}), \boldsymbol{s}_h^{k-1})\|_0^2 \le C(\Delta t) h^{2k} \|\boldsymbol{u}\|_{L^\infty(H^2)}^2 \int_{t_{k-2}}^{t_{k-1}} \|\boldsymbol{u}_t\|_{k+1}^2 \, dt$$

and

$$\|B(\boldsymbol{u}^{k-1} - \boldsymbol{s}_h^{k-1}, \boldsymbol{s}_h^k - \boldsymbol{s}_h^{k-1})\|_0^2 \le C(\Delta t) h^{2k} \|\boldsymbol{u}\|_{L^\infty(H^{k+1})}^2 \int_{t_{k-1}}^{t_k} \|\boldsymbol{u}_t\|_2^2 \, dt.$$

For the fifth one, by writing

$$\|B(\boldsymbol{u}^{k-1} - \boldsymbol{u}^{k-2}, \boldsymbol{u}^{k-1} - \boldsymbol{s}^{k-1})\|_0^2 \le C \|d_t \boldsymbol{u}^{k-1}\|_\infty^2 \|\nabla(\boldsymbol{u}^{k-1} - \boldsymbol{s}^{k-1})\|_0^2,$$

we have

$$\|B(\boldsymbol{u}^{k-1}-\boldsymbol{u}^{k-2},\boldsymbol{u}^{k-1}-\boldsymbol{s}^{k-1})\|_0^2 \le C(\Delta t)h^{2k}\|\boldsymbol{u}\|_{L^\infty(H^{k+1})}^2\int_{t_{k-2}}^{t_{k-1}}\|\boldsymbol{u}_t\|_2^2\,dt$$

and arguing similarly with the sixth one,

$$\|B(\boldsymbol{u}^{k-1},d_t(\boldsymbol{u}^k-\boldsymbol{s}_h^k)\|_0^2 \le C(\Delta t)h^{2k}\|\boldsymbol{u}\|_{L^\infty(H^2)}^2\int_{t_{k-1}}^{t_k}\|\boldsymbol{u}_t\|_{k+1}^2\,dt.$$

Now, multiplying by Δt the above expressions and summing from $k=2$ onwards the proof is finished. □

B Tables for Section 4.2

We present detailed tables corresponding to the numerical experiment in Section 4.2. For the convenience of the reader, reference values are shown at the bottom line in every table. In all tables, the value of Δt_0 is

$$\Delta t_0 = \frac{1}{640}.$$

Reference values are taken from [35].

In Table 1, for the second finest mesh that we used, we compare results for different values of μ. It can be seen that for $\mu = 0.01$ there is a better coincidence of computed values and reference ones, especially for the lift coefficient c_l. The most accurate computation of the drag coefficient corresponds to $\mu = 0$.

μ	Δt	$t_{d,\max}$	$c_{d,\max}$	$t_{l,\max}$	$c_{l,max}$	$\Delta p(8)$
0	$\Delta t_0/4$	3.9320	2.9507	6.7602	0.0476	-0.1179
0	$\Delta t_0/8$	3.9320	2.9507	6.7602	0.0531	-0.1164
0	$\Delta t_0/16$	3.9320	2.9507	6.7601	0.0561	-0.1156
0	$\Delta t_0/32$	3.9320	2.9507	6.7600	0.0577	-0.1152
0.001	$\Delta t_0/4$	3.9324	2.9507	6.8141	0.1503	-0.1024
0.001	$\Delta t_0/8$	3.9324	2.9507	6.8057	0.1638	-0.1041
0.001	$\Delta t_0/16$	3.9323	2.9507	6.8009	0.1709	-0.1050
0.001	$\Delta t_0/32$	3.9324	2.9507	6.7984	0.1745	-0.1055
0.01	$\Delta t_0/8$	3.9334	2.9528	5.9061	0.4618	-0.1104
0.01	$\Delta t_0/16$	3.9334	2.9528	5.9026	0.4698	-0.1100
0.01	$\Delta t_0/32$	3.9335	2.9528	5.9009	0.4739	-0.1097
0.01	$\Delta t_0/64$	3.9335	2.9528	5.9001	0.4759	-0.1096
0.1	$\Delta t_0/4$	3.9375	2.9582	5.4102	0.5519	-0.0987
0.1	$\Delta t_0/8$	3.9383	2.9584	5.4053	0.5668	-0.0987
0.1	$\Delta t_0/16$	3.9387	2.9585	5.4028	0.5744	-0.0988
0.1	$\Delta t_0/32$	3.9389	2.9585	5.4016	0.5782	-0.0988
1	$\Delta t_0/4$	3.9457	2.9832	5.4367	0.5512	-0.1129
1	$\Delta t_0/8$	3.9453	2.9841	5.4311	0.5643	-0.0932
1	$\Delta t_0/16$	3.9456	2.9843	5.4284	0.5724	-0.0898
1	$\Delta t_0/32$	3.9458	2.9843	5.4270	0.5761	-0.0890
ref.	values	3.9362	2.9509	5.6931	0.4780	-0.1116

Table 1: Results for mesh with 16961 degrees freedom and different values of μ.

dgf	Δt	$t_{d,\max}$	$c_{d,\max}$	$t_{l,\max}$	$c_{l,max}$	$\Delta p(8)$
2057	Δt_0	3.9234	2.9348	0.9172	0.0010	-0.1310
2057	$\Delta t_0/2$	3.9234	2.9347	0.9180	0.0010	-0.1310
2057	$\Delta t_0/4$	3.9234	2.9347	0.9184	0.0010	-0.1310
2057	$\Delta t_0/8$	3.9234	2.9347	0.9186	0.0010	-0.1310
4208	Δt_0	3.9297	2.9597	0.9313	0.0012	-0.1290
4208	$\Delta t_0/2$	3.9297	2.9597	0.9328	0.0012	-0.1290
4208	$\Delta t_0/4$	3.9293	2.9597	0.9336	0.0012	-0.1290
4208	$\Delta t_0/8$	3.9295	2.9597	0.9340	0.0012	-0.1290
7709	Δt_0	3.9297	2.9514	0.9438	0.0012	-0.1281
7709	$\Delta t_0/2$	3.9305	2.9514	0.9453	0.0012	-0.1281
7709	$\Delta t_0/4$	3.9301	2.9514	0.9457	0.0012	-0.1281
7709	$\Delta t_0/8$	3.9303	2.9514	0.9457	0.0012	-0.1281
16961	$\Delta t_0/4$	3.9320	2.9507	6.7602	0.0476	-0.1179
16961	$\Delta t_0/8$	3.9320	2.9507	6.7602	0.0531	-0.1164
16961	$\Delta t_0/16$	3.9320	2.9507	6.7601	0.0561	-0.1156
16961	$\Delta t_0/32$	3.9320	2.9507	6.7600	0.0577	-0.1152
46265	$\Delta t_0/4$	3.9320	2.9504	5.8359	0.3594	-0.1008
46265	$\Delta t_0/8$	3.9322	2.9504	5.8309	0.3778	-0.1002
46265	$\Delta t_0/16$	3.9323	2.9504	5.8281	0.3871	-0.1000
46265	$\Delta t_0/32$	3.9323	2.9504	5.8268	0.3918	-0.0999
ref.	values	3.9362	2.9509	5.6931	0.4780	-0.1116

Table 2: Results for $\mu = 0$ on meshes with increasing number of degrees of freedom.

dgf	Δt	$t_{d,\max}$	$c_{d,\max}$	$t_{l,\max}$	$c_{l,\max}$	$\Delta p(8)$
2057	Δt_0	3.9250	2.9313	6.8344	0.0151	-0.1291
2057	$\Delta t_0/2$	3.9242	2.9312	6.8328	0.0218	-0.1280
2057	$\Delta t_0/4$	3.9246	2.9312	6.8328	0.0263	-0.1269
2057	$\Delta t_0/8$	3.9244	2.9312	6.8330	0.0289	-0.1262
4208	Δt_0	3.9250	2.9595	7.6953	0.0751	-0.1056
4208	$\Delta t_0/2$	3.9258	2.9595	6.4602	0.1082	-0.0967
4208	$\Delta t_0/4$	3.9254	2.9595	6.4563	0.1318	-0.0973
4208	$\Delta t_0/8$	3.9256	2.9596	6.4535	0.1460	-0.0988
7709	Δt_0	3.9297	2.9524	6.8531	0.2189	-0.1034
7709	$\Delta t_0/2$	3.9297	2.9524	6.1617	0.2800	-0.1096
7709	$\Delta t_0/4$	3.9301	2.9524	6.1461	0.3235	-0.1108
7709	$\Delta t_0/8$	3.9303	2.9524	6.1379	0.3465	-0.1106
16961	$\Delta t_0/8$	3.9334	2.9528	5.9061	0.4618	-0.1104
16961	$\Delta t_0/16$	3.9334	2.9528	5.9026	0.4698	-0.1100
16961	$\Delta t_0/32$	3.9335	2.9528	5.9009	0.4739	-0.1097
16961	$\Delta t_0/64$	3.9335	2.9528	5.9001	0.4759	-0.1096
46265	$\Delta t_0/4$	3.9340	2.9517	5.7559	0.4753	-0.1062
46265	$\Delta t_0/8$	3.9344	2.9518	5.7516	0.4899	-0.1072
46265	$\Delta t_0/16$	3.9346	2.9518	5.7492	0.4973	-0.1076
46265	$\Delta t_0/32$	3.9346	2.9518	5.7480	0.5010	-0.1079
ref.	values	3.9362	2.9509	5.6931	0.4780	-0.1116

Table 3: Results for $\mu = 0.01$ on meshes with increasing number of degrees of freedom.